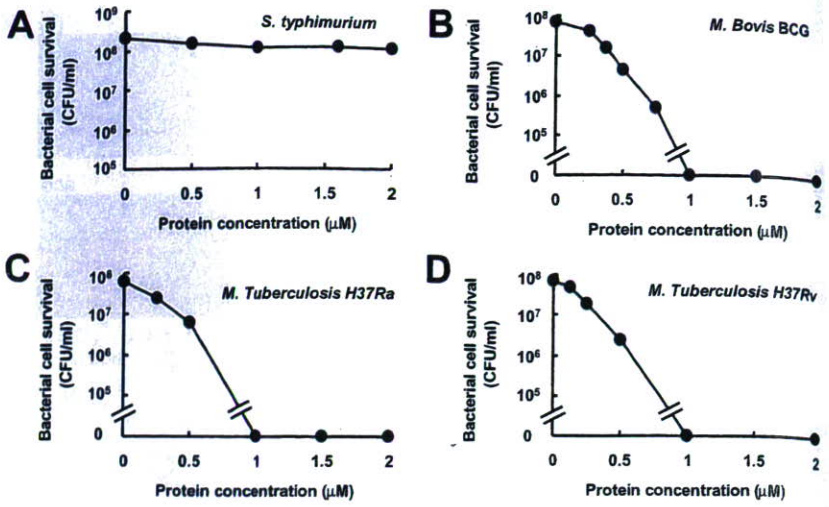

FIGURE 2. Mouse recombinant SLPI inhibits in vitro BCG and *M. tuberculosis* growth. *A*, *S. typhimurium* (5×10^7 CFU/ml) were incubated with SLPI for 2 h and plated on LB agar plates. *B–D*, BCG (*B*), *M. tuberculosis* H37Ra (*C*), or *M. tuberculosis* H37Rv (*D*; 5×10^7 CFU/ml) were incubated with increasing concentrations of recombinant mouse SLPI for 24 h and then plated on 7H10 agar plates.

Bronchoalveolar lavage fluid (BALF)

Mice were intratracheally administered 4×10^5 CFU of BCG suspended in 30 μl of PBS. BALF was collected at the indicated periods. To obtain alveolar macrophages, BALF was centrifuged at 2000 × g for 2 min and the pellet was resuspended in RPMI 1640 containing 4% FBS. The cell count of alveolar macrophages was $\sim 1 \times 10^5$ cells/mouse. To eliminate contamination by bacteria, alveolar macrophages were cultured with 50 U/ml penicillin and 50 μg/ml streptomycin for 16 h, washed five times, and infected with 5×10^7 CFU/well of BCG without penicillin and streptomycin.

Preparation of recombinant SLPI protein and variants

PCR-amplified mouse SLPI cDNA fragments were inserted into pGEX-6P-1 (Amersham Biosciences). pGEX-6P-1 containing mouse SLPI cDNA was transformed into *Escherichia coli* Rosetta-gami B (DE 3). Expression of GST-SLPI fusion proteins was induced by the addition of 1 mM isopropyl-1-thio-β-D-galactoside, and the expressed fusion proteins were purified using glutathione-Sepharose 4B (Amersham Biosciences) according to the manufacturer's instructions. The purified proteins were incubated with PreScission Protease (Amersham Biosciences) at 4°C for 16 h to cleave the GST tag and then purified with glutathione-Sepharose 4B.

Antibacterial activity

Mid-log phase *Salmonella typhimurium* were diluted with PBS containing 1% Luria-Bertani (LB) to give $\sim 5 \times 10^7$ CFU/ml. A final volume of 250 μl was used to examine the antibacterial activities of proteins. After incubation for 2 h, *S. typhimurium* were plated onto LB agar plates. Colonies were counted (CFU/ml) after overnight incubation at 37°C.

Antimycobacterial activity

M. tuberculosis and BCG were grown in Middlebrook 7H9-ADC medium at 37°C with vigorous agitation. After 7 days of incubation, rapidly growing mycobacteria were harvested by centrifugation and adjusted to 5×10^7 CFU/ml in 7H9-ADC medium. After incubation of the mycobacteria with the indicated concentrations of proteins for 24 h at 37°C, serial 20-fold dilutions were conducted in PBS. Aliquots (50 μl) of the dilutions were plated on Middlebrook 7H10 agar plates and incubated at 37°C for 21–28 days. Colonies were counted (CFU/ml) at intervals until no new colonies appeared.

Protein-binding assay

SLPI and BSA were labeled with 5-(and 6-)carboxyfluorescein-*N*-hydroxysuccinimide ester (FLUOS; Roche Diagnostics) as described previously (30). Briefly, 400 μg/ml SLPI or BSA was mixed with 0.096 mg of FLUOS in 1 ml of PBS for 2 h at room temperature. Nonreacted FLUOS was separated by gel filtration using a Sephadex G25 column (Amersham Biosciences). The labeled SLPI or BSA was then incubated with BCG, and the OD at 630 nm was adjusted to 0.2. After 30 min of incubation at 37°C, BCG were washed three times with 7H9 medium containing 0.05% Tween 80. Protein-BCG reactions were detected by confocal laser microscopy (Zeiss).

Scanning electron microscopy

After culture with or without 1 μM SLPI for the indicated times, BCG cultures were fixed with 5% glutaraldehyde, postfixed with 1% osmium tetroxide, dehydrated with ethyl alcohol, treated with isoamyl acetate to replace the alcohol, dried with liquid CO_2 in a critical-point apparatus (HCP-2; Hitachi), and coated with Pt-Pd by ion sputtering (Hitachi) in ion-distilled water. The specimens were analyzed using S-4700 scanning electron microscope (Hitachi), operated at 10 kV.

Outer membrane permeabilization assay

The ability of proteins to permeabilize the outer membranes of BCG was investigated using 1-*N*-phenylnaphthylamine (NPN; Wako Pure Chemical Industries) as described previously (31). Briefly, BCG were suspended in 5 mM HEPES (pH 7.4) containing 10 μM NPN to an OD at 590 nm of 0.15. After incubation at 37°C for 30 min, proteins were added and the fluorescence of NPN was monitored. The excitation wavelength used was 340 nm, and the emission wavelength was 425 nm. The experiment was conducted at 37°C.

Generation of $Slpi^{-/-}$ *mice*

The *Slpi* gene was isolated from genomic DNA extracted from embryonic stem cells (E14.1) by PCR using TaKaRa LA *Taq*. The targeting vector was constructed by replacing a 1.2-kb fragment containing exons 2–4 with a neomycin-resistance gene cassette (*neo*) driven by the PGK promoter and inserting a HSV thymidine kinase into the genomic fragment for negative selection. After transfection of the targeting vector into embryonic stem cells, colonies resistant to both G418 and ganciclovir were selected and screened by PCR and Southern blotting. Homologous recombinants were microinjected into blastocysts of C57BL/6 female mice and heterozygous F_1 progenies were intercrossed to obtain $Slpi^{-/-}$ mice.

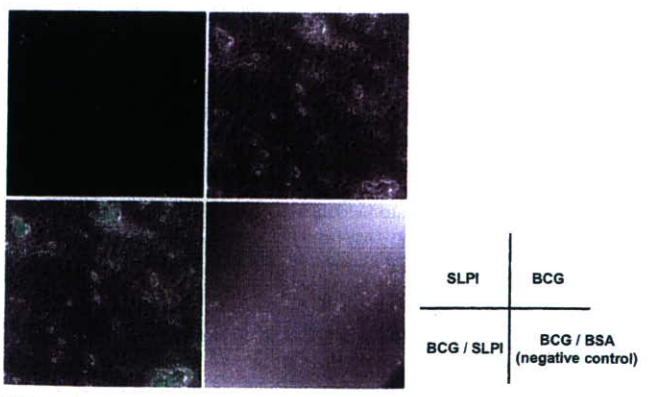

FIGURE 3. SLPI associates with BCG. SLPI and BSA were labeled with FLUOS (Roche). Labeled proteins were incubated with BCG for 30 min, and analyzed by fluorescence microscopy.

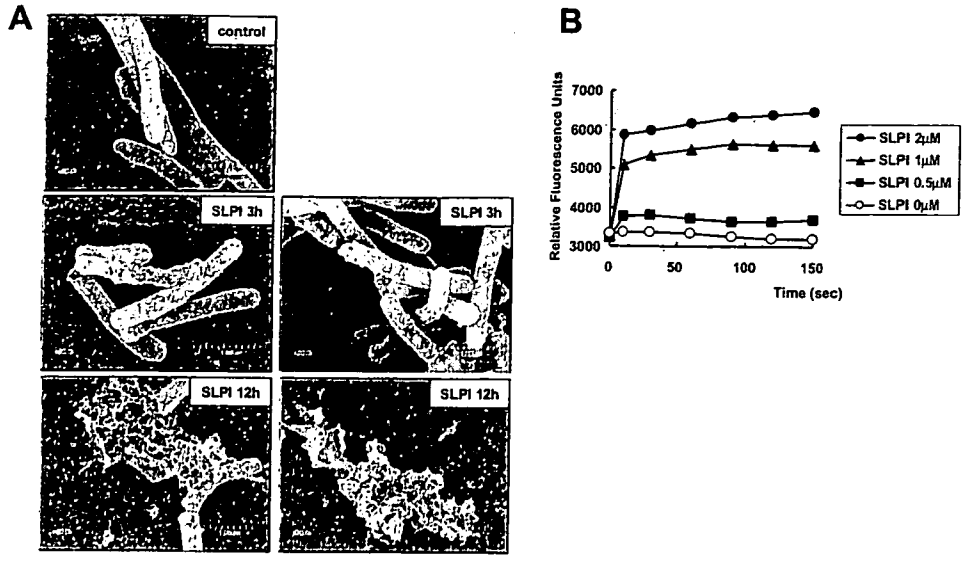

FIGURE 4. SLPI disrupts the BCG cell membrane. *A*, BCG was incubated with or without SLPI for the indicated periods and observed with scanning electron microscopy. *B*, The indicated concentrations of SLPI were added to a BCG suspension containing NPN, and the NPN fluorescence was monitored for the indicated periods. Representative data of three independent experiments are shown.

Slpi$^{-/-}$ mice were backcrossed to C57BL/6 mice for five generations, and *Slpi*$^{-/-}$ and their wild-type littermates from these intercrosses were used for experiments at 6–8 wk of age. All animal experiments were conducted in accordance with the guidelines of the Animal Care and Use Committee of Kyushu University.

In vivo infection

For intratracheal infection, 4×10^5 CFU of *M. tuberculosis* suspended in 30 μl of sterile PBS were administered intratracheally. For i.v. infection, 4×10^5 CFU of *M. tuberculosis* suspended in 100 μl of sterile PBS were administered i.v. At 3 wk after infection, homogenates of the lungs and spleen were plated on 7H10 agar plates. For histological examination, 1×10^7 CFU of *M. tuberculosis* suspended in 30 μl of sterile PBS were administered intratracheally. At 5 days after infection, the lungs were fixed in 4% formalin, embedded in paraffin, cut into sections, and stained with H&E.

Results

SLPI expression in the lungs of BCG-infected mice

To assess the roles of SLPI in mycobacterial infection, we first analyzed SLPI expression in the lungs of mice intratracheally infected with *M. bovis* BCG. Total RNA was extracted from the lungs after 2, 7, and 14 days of infection and analyzed for SLPI mRNA expression by real-time qPCR (Fig. 1*A*). Expression of SLPI mRNA was increased by ~9-fold after 2 days of infection, but decreased thereafter. Next, we analyzed pulmonary cell types expressing SLPI by immunohistochemical analysis (Fig. 1, *B* and *C*). SLPI was detected in bronchial epithelial cells before BCG infection (Fig. 1*B, upper micrograph*). After 2 days of BCG infection, increased amounts of SLPI expression were observed, and mainly localized at the apical side of bronchial epithelial cells (Fig. 1*B, lower micrograph*). This prompted us to investigate whether SLPI was secreted into the alveolar space after BCG infection. Accordingly, BALF was collected from BCG-infected mice and analyzed for SLPI protein expression by Western blotting (Fig. 1*D*). SLPI was not detected in BALF from uninfected mice. After 2 days of BCG infection, SLPI was abundantly detected in BALF from infected mice, indicating that SLPI was secreted into the alveolar space during the early phase of mycobacterial infection. In addition to bronchial epithelial cells, SLPI was expressed in cells of the alveolar area (Fig. 1*C*). Therefore, we isolated type II alveolar epithelial cells (AEC) and alveolar macrophages and analyzed their SLPI expression levels after BCG infection. Since AEC are difficult to culture in vitro, we took advantage of transgenic mice harboring a temperature-sensitive mutation of the SV40 large tumor Ag gene under the control of an IFN-γ-inducible H-2K^b promoter element (32, 33). Using these mice, we successfully established AEC lines expressing surfactant protein C (data not shown).

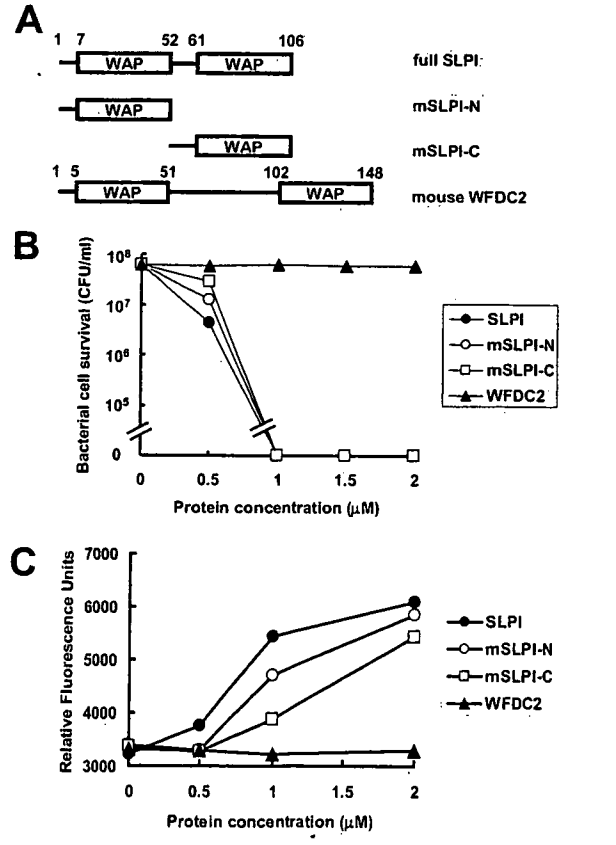

FIGURE 5. A single WAP domain in SLPI is sufficient to inhibit BCG growth. *A*, The deletion mutant constructs mSLPI-N and mSLPI-C lack the C-terminal and N-terminal portions, respectively. White boxes denote WAP domains. *B*, BCG (5×10^7 CFU/ml) was incubated with increasing concentrations of the deletion mutants (mSLPI-N and mSLPI-C) or WFDC2 for 24 h and then plated on 7H10 agar plates. *C*, The indicated concentrations of the deletion mutants (mSLPI-N and mSLPI-C) or WFDC2 were added to BCG suspensions containing NPN. The peak of NPN fluorescence within 150 s was plotted. Representative data of three independent experiments are shown.

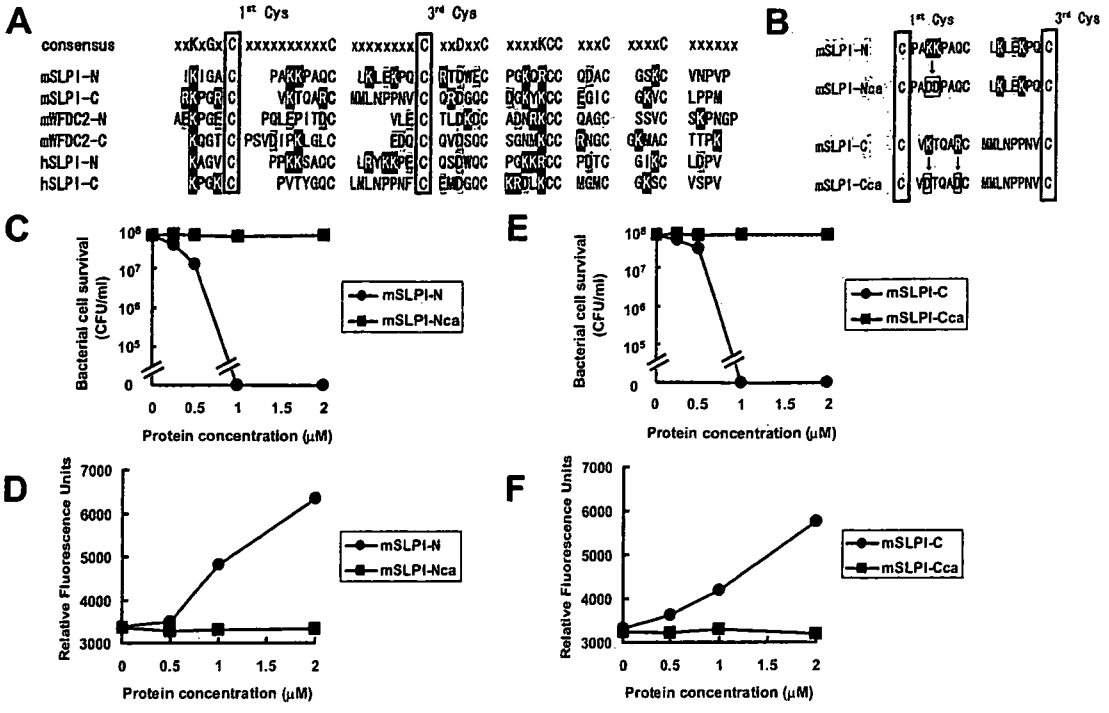

FIGURE 6. Cationic amino acids are responsible for the antimycobacterial activity of SLPI. *A*, Comparison of the WAP domain of SLPI with the WAP domains of other proteins. The consensus amino acid sequence of the WAP domain is shown at the *top* of the protein sequences. Black- and gray-boxed amino acids indicate cationic and anionic amino acids, respectively. Two conserved cysteine residues (first cysteine and third cysteine) are boxed. *B*, Amino acid sequences of the mSLPI-N (mSLPI-Nca) and mSLPI-C (mSLPI-Cca) mutants. *C* and *E*, BCG (5×10^7 CFU/ml) was incubated with increasing concentrations of mSLPI-Nca (*C*) and mSLPI-Cca (*E*) for 24 h and then plated on 7H10 agar plates. *D* and *F*, The indicated concentrations of mSLPI-Nca (*D*) and mSLPI-Cca (*F*) were added to BCG cultures containing NPN. The peak of NPN fluorescence within 150 s was plotted.

AEC were infected with BCG and analyzed for SLPI mRNA expression (Fig. 1*E*). SLPI mRNA expression was gradually induced after BCG infection and peaked after 36 h of infection. AEC have the ability to secrete several effector molecules into the alveolar space. Therefore, we analyzed the SLPI protein levels in culture supernatants from BCG-infected AEC by Western blotting (Fig. 1*F*). SLPI protein was not detected in supernatants from uninfected AEC, but was clearly detected in supernatants after 24 h of BCG infection. Next, isolated alveolar macrophages were infected with BCG and analyzed for SLPI mRNA expression (Fig. 1*G*). BCG infection resulted in an increase in SLPI mRNA expression. Taken together, mycobacterial infection induces the production and secretion of SLPI into the alveolar space by bronchial and type II alveolar epithelial cells as well as alveolar macrophages in the lung.

SLPI-mediated inhibition of mycobacterial growth

Several previous reports have described antimicrobial activities of SLPI against Gram-positive bacteria, Gram-negative bacteria, HIV, and fungi (18–20). However, SLPI needs to be present at high concentrations (>10 μM) for effective inhibition of microbial growth, particularly *S. typhimurium* and *E. coli* (18, 34). Indeed, addition of 2 μM recombinant mouse SLPI only moderately decreased the growth of *S. typhimurium* (Fig. 2*A*). In sharp contrast to the mild inhibition of *S. typhimurium* growth, addition of lower concentrations of mouse SLPI to BCG cultures dramatically reduced the number of CFU (Fig. 2*B*). Growth of BCG was almost completely inhibited by the addition of 1 μM SLPI. A similar inhibitory effect was observed on the growth of *M. tuberculosis* H37Ra and H37Rv (Fig. 2, *C* and *D*). These findings indicate that SLPI has a more potent antimicrobial activity against mycobacteria than against *S. typhimurium*.

Disruption of the BCG cell wall structure by SLPI

Next, we investigated the mechanism of the antimycobacterial activity of SLPI. First, fluorescence-labeled SLPI was incubated with BCG and analyzed by confocal laser microscopy (Fig. 3). BCG and labeled SLPI were colocalized, suggesting that SLPI becomes associated with BCG. We then examined the morphological effects of SLPI on BCG. BCG was incubated with or without SLPI and analyzed by scanning electron microscopy (Fig. 4*A*). BCG exposed to SLPI for 3 h showed pronounced surface blebbing. After 12 h of incubation, many of BCG were collapsed and few live BCG had rough and irregular membrane surfaces. Next, BCG was subjected to an outer membrane permeabilization assay using a fluorescent dye that is weakly fluorescent in aqueous environments but becomes strongly fluorescent in the hydrophobic environment within the cell membrane (Fig. 4*B*). Addition of SLPI caused rapid increases in fluorescence in a dose-dependent manner. These results suggest that SLPI directly associates with mycobacteria, and disrupts the cell wall structure.

Critical role of cationic amino acids in SLPI in its antimycobacterial activity

We next investigated the critical domain involved in the antimycobacterial activity of SLPI. SLPI has two WAP domains (Fig. 5*A*). Several serine protease inhibitors possessing a single WAP domain, such as Eppin, Elafin, SWAM1, and SWAM2, have antimicrobial activities against bacteria such as *E. coli* and *Staphylococcus aureus* (8, 21, 22). To investigate whether each of the WAP domains of mouse SLPI is sufficient to exert antimycobacterial activity, two deletion mutants of SLPI, mSLPI-N and

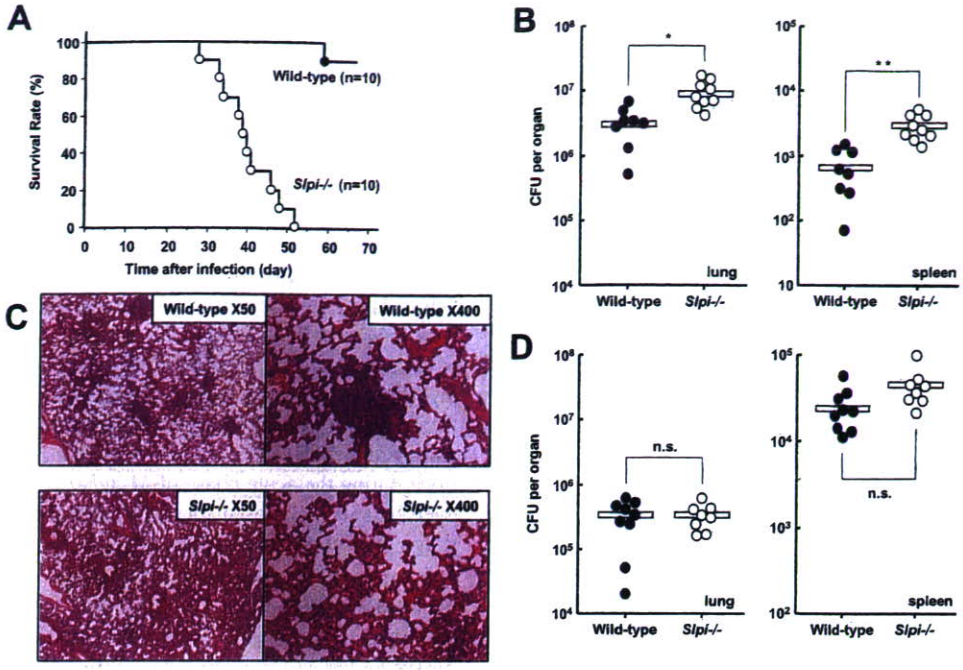

FIGURE 7. *Slpi*$^{-/-}$ mice are highly susceptible to *M. tuberculosis* infection. *A*, *M. tuberculosis* (4×10^5 CFU) were intratracheally infected into wild-type and *Slpi*$^{-/-}$ mice and their survival was monitored. *B*, *M. tuberculosis* (4×10^5 CFU) were intratracheally infected into wild-type and *Slpi*$^{-/-}$ mice. At 3 wk after infection, homogenates of the lungs and spleen were plated on 7H10 agar plates and the CFU titers were counted. Symbols represent individual mice and bars represent the mean of CFU numbers. Statistical analyses were performed using Student's *t* test: *, $p < 0.005$ and **, $p < 0.0005$, significant difference between wild-type and *Slpi*$^{-/-}$ mice. *C*, H&E staining of representative lung tissues from wild-type and *Slpi*$^{-/-}$ mice on day 5 after intratracheal infection with *M. tuberculosis*. *D*, *M. tuberculosis* (4×10^5 CFU) were i.v. infected into wild-type and *Slpi*$^{-/-}$ mice. At 3 wk after infection, homogenates of the lungs and spleen were plated on 7H10 agar plates, and the CFU titers were counted. Symbols represent individual mice and bars represent the mean of CFU numbers. Statistical analyses were performed using Student's *t* test. n.s., Not significant

mSLPI-C, were generated (Fig. 5*A*). mSLPI-N contained the N-terminal WAP domain, while mSLPI-C contained the C-terminal WAP domain. Both mSLPI-N and mSLPI-C inhibited BCG growth, although their efficiencies were slightly decreased compared with that of full-length SLPI (Fig. 5*B*). Similarly, mSLPI-N and mSLPI-C both induced permeabilization of the outer membrane of BCG with slightly lower efficacies (Fig. 5*C*). These results imply that each WAP domain of mouse SLPI exhibits antimycobacterial activity by disrupting the mycobacterial cell wall structure. WFDC2 is a secreted protein possessing two WAP domains (Fig. 5*A*) (35). However, recombinant mouse WFDC2 had no effect on mycobacterial growth and did not induce permeabilization of the BCG cell membrane, indicating that not all WAP domain-containing proteins have antimicrobial activities (Fig. 5, *B* and *C*). In addition, the N-terminal, but not the C-terminal, WAP domain of human SLPI has been shown to mediate its antimicrobial activities against *E. coli* and *S. aureus* (18). Therefore, we compared the amino acid sequences of the WAP domains of mouse and human SLPI as well as mouse WFDC2 (Fig. 6*A*). The C-terminal regions were conserved among all of the WAP domains. However, the sequences between the first and third cysteine residues were less conserved. In particular, when we examined the sequences between the first and second cysteine residues, we noted that the WAP domains possessing antimycobacterial activities (mSLPI-N, mSLPI-C, and hSLPI-N) contained two or more cationic amino acids, whereas the WAP domains with no antimycobacterial activities (mWFDC2-N, mWFDC2-C, and hSLPI-C) had one or zero cationic acids and instead contained anionic amino acids. Therefore, we produced mSLPI-N (mSLPI-Nca) and mSLPI-C (mSLPI-Cca) mutants, in which the two cationic amino acids were changed to the anionic amino acid aspartic acid (Fig. 6*B*). Neither mSLPI-Nca nor mSLPI-Cca was able to inhibit BCG growth or permeabilize the cell membrane (Fig. 6, *C–F*). These results suggest that the cationic acids of mouse SLPI are responsible for its potent antimycobacterial activities.

High susceptibility of SLPI-deficient mice to M. tuberculosis *infection*

In the next experiment, we assessed the physiological roles of SLPI during mycobacterial infection by generating mice lacking SLPI (*Slpi*$^{-/-}$ mice) via gene targeting (data not shown). First, wild-type and *Slpi*$^{-/-}$ mice were intratracheally infected with *M. tuberculosis* H37Ra, and monitored for their survival (Fig. 7*A*). All *Slpi*$^{-/-}$ mice died within 8 wk of infection at a dose that almost all wild-type mice survived for >9 wk. Next, we counted CFU numbers in the lungs and spleen after 3 wk of infection (Fig. 7*B*). The CFU titers of *M. tuberculosis* in both tissues were higher for *Slpi*$^{-/-}$ mice than that for wild-type mice. The histopathological changes in the lungs after 5 days of *M. tuberculosis* infection were also analyzed (Fig. 7*C*). In wild-type mice, the formation of several small granulomas was observed. In contrast, granulomatous changes were induced to a lesser extent in *Slpi*$^{-/-}$ mice and rather diffuse cell infiltration was observed instead. Next, mice were i.v. infected with *M. tuberculosis*, and the CFU numbers in the lungs and spleen were counted after 3 wk of infection (Fig. 7*D*). The CFU titers were not as dramatically increased in both tissues of *Slpi*$^{-/-}$ mice compared with the corresponding titers in the tissues of wild-type mice, indicating that *Slpi*$^{-/-}$ mice are not highly susceptible to i.v. *M. tuberculosis* infection. Taken together, these findings indicate that *Slpi*$^{-/-}$ mice are highly vulnerable to *M. tuberculosis* infection via the respiratory route.

Discussion

In the present study, we analyzed the roles of mouse SLPI in host defense against mycobacteria. During the early phase of respiratory mycobacterial infection, SLPI was produced and secreted into the alveolar space by bronchial and type II alveolar epithelial cells as well as alveolar macrophages. Recombinant mouse SLPI inhibited the growth of mycobacteria more effectively than it inhibited the growth of Gram-negative bacteria. The SLPI-mediated inhibition of mycobacterial growth was attributable to disruption of the mycobacterial cell wall structure. Furthermore, *Slpi*$^{-/-}$ mice were highly susceptible to pulmonary *M. tuberculosis* infection, highlighting a mandatory role for mouse SLPI in the host defense against *M. tuberculosis* infection. Thus, mouse SLPI is a critical antimycobacterial molecule that acts during the early phase of mycobacterial infection at the respiratory mucosal surface.

Similar structural changes to those observed in SLPI-treated mycobacterial cell walls were induced in several bacteria and *M. tuberculosis* treated with the antimicrobial peptides defensins, which permeabilize microbial membranes (36, 37). We further identified the critical elements for the potent antimycobacterial activity of mouse SLPI. It has been proposed that defensins containing positively charged amino acid residues associate with microorganisms by targeting the surface-exposed negatively charged phospholipid head groups in the microbial membrane (37). Indeed, mutations that change arginine to aspartic acid can attenuate the bactericidal activity of the α-defensin cryptdin-4 (38). Therefore, we supposed that SLPI, which has similar effects on mycobacterial membranes to defensins, also associates with negatively charged mycobacterial membranes through its positively charged amino acid residues. Consistent with this hypothesis, the sequences between the first and second conserved cysteine residues of the WAP domains are not conserved. Moreover, there are several positively charged amino acids (lysine and arginine) in these regions of the WAP domains that possess antimicrobial activities, whereas the regions without any antimicrobial activities contain one or zero positively charged amino acids. Furthermore, structural studies have revealed that the region between the first and second conserved cysteine residues is exposed on the outside of the molecule, thereby enabling this region to associate with microbial membranes (39, 40). Indeed, mutations of the cationic amino acid residues within this region resulted in elimination of the antimycobacterial activity. Thus, mouse SLPI exhibits antimycobacterial activity in quite a similar manner to that of defensins.

In comparison to SLPI, higher concentrations of other serine protease inhibitors containing a WAP domain are required to inhibit microbial growth (8, 21, 22). Recombinant human SLPI is less effective at inhibiting the growth of mycobacteria and *S. typhimurium* (our unpublished data). These differential properties may be attributable to structural differences in the WAP domains, which mediate the antimicrobial activity. SLPI has two WAP domains, whereas other serine protease inhibitors, such as Eppin, Elafin, and SWAMs, have only a single WAP domain. In the case of human SLPI, only the N-terminal WAP domain exhibits antimicrobial activity (18). In addition, only the N-terminal WAP domain of human SLPI contains critical cationic acid residues. The presence of two WAP domains possessing antimicrobial activity may be responsible for the high potency of mouse SLPI for mycobacterial growth inhibition.

Mouse SLPI inhibited mycobacterial growth at profoundly lower concentrations than those required to inhibit the growth of *S. typhimurium* or other microorganisms (18–20). It remains unclear how SLPI becomes more specifically targeted toward mycobacteria. Differential antimicrobial properties against distinct microorganisms have not been reported in the case of defensins. Therefore, SLPI, which has multifunctional properties, may have an unknown strategy for specifically recognizing mycobacteria.

The in vitro findings demonstrating that mouse SLPI inhibits mycobacterial growth were further strengthened by in vivo studies using *Slpi*$^{-/-}$ mice. *Slpi*$^{-/-}$ mice were highly susceptible to pulmonary *M. tuberculosis* infection, but not to i.v. infection. In accordance with this finding, SLPI protein was abundantly detected in the alveolar space after pulmonary BCG infection, but was not detected in sera from mice after i.v. BCG infection (our unpublished data). Therefore, high concentrations of SLPI are supposed to be secreted into the alveolar space during the early phase of respiratory infection with *M. tuberculosis*, thereby promptly killing the mycobacteria before they can invade the lung tissues through the epithelial barrier. Given that mouse SLPI has potent antimycobacterial activities, it would be a good candidate for treatment during the acute phase of *M. tuberculosis* infection and may even be able to be used for the treatment of patients with multidrug-resistant *M. tuberculosis*.

Acknowledgments

We thank S. Ehrt and A. Ding for helpful discussions, Y. Yamada and K. Takeda for technical assistance, and M. Kurata for secretarial assistance.

Disclosures

The authors have no financial conflict of interest.

References

1. Kaufmann, S. H. 2006. Tuberculosis: back on the immunologists' agenda. *Immunity* 24: 351–357.
2. North, R. J., and Y. J. Jung. 2004. Immunity to tuberculosis. *Annu. Rev. Immunol.* 22: 599–623.
3. Fremond, C. M., V. Yeremeev, D. M. Nicolle, M. Jacobs, V. F. Quesniaux, and B. Ryffel. 2004. Fatal *Mycobacterium tuberculosis* infection despite adaptive immune response in the absence of MyD88. *J. Clin. Invest.* 114: 1790–1799.
4. Quesniaux, V., C. Fremond, M. Jacobs, S. Parida, D. Nicolle, V. Yeremeev, F. Bihl, F. Erard, T. Botha, M. Drennan, et al. 2004. Toll-like receptor pathways in the immune responses to mycobacteria. *Microbes Infect.* 6: 946–959.
5. Gerritsen, J. 2000. Host defence mechanisms of the respiratory system. *Paediatr. Respir. Rev.* 1: 128–134.
6. Clauss, A., H. Lilja, and A. Lundwall. 2005. The evolution of a genetic locus encoding small serine proteinase inhibitors. *Biochem. Biophys. Res. Commun.* 333: 383–389.
7. Eisenberg, S. P., K. K. Hale, P. Heimdal, and R. C. Thompson. 1990. Location of the protease-inhibitory region of secretory leukocyte protease inhibitor. *J. Biol. Chem.* 265: 7976–7981.
8. Hagiwara, K., T. Kikuchi, Y. Endo, Huqun, K. Usui, M. Takahashi, N. Shibata, T. Kusakabe, H. Xin, S. Hoshi, et al. 2003. Mouse SWAM1 and SWAM2 are antibacterial proteins composed of a single whey acidic protein motif. *J. Immunol.* 170: 1973–1979.
9. Abe, T., N. Kobayashi, K. Yoshimura, B. C. Trapnell, H. Kim, R. C. Hubbard, M. T. Brewer, R. C. Thompson, and R. G. Crystal. 1991. Expression of the secretory leukoprotease inhibitor gene in epithelial cells. *J. Clin. Invest.* 87: 2207–2215.
10. Hiemstra, P. S., S. van Wetering, and J. Stolk. 1998. Neutrophil serine proteinases and defensins in chronic obstructive pulmonary disease: effects on pulmonary epithelium. *Eur. Respir. J.* 12: 1200–1208.
11. Schiessler, H., E. Fink, and H. Fritz. 1976. Acid-stable proteinase inhibitors from human seminal plasma. *Methods Enzymol.* 45: 847–859.
12. Vogelmeier, C., R. C. Hubbard, G. A. Fells, H. P. Schnebli, R. C. Thompson, H. Fritz, and R. G. Crystal. 1991. Anti-neutrophil elastase defense of the normal human respiratory epithelial surface provided by the secretory leukoprotease inhibitor. *J. Clin. Invest.* 87: 482–488.
13. Wingens, M., B. H. van Bergen, P. S. Hiemstra, J. F. Meis, I. M. van Vlijmen-Willems, P. L. Zeeuwen, J. Mulder, H. A. Kramps, F. van Ruissen, and J. Schalkwijk. 1998. Induction of SLPI (ALP/HUSI-I) in epidermal keratinocytes. *J. Invest. Dermatol.* 111: 996–1002.
14. Gauthier, F., U. Fryksmark, K. Ohlsson, and J. G. Bieth. 1982. Kinetics of the inhibition of leukocyte elastase by the bronchial inhibitor. *Biochim. Biophys. Acta* 700: 178–183.
15. Thompson, R. C., and K. Ohlsson. 1986. Isolation, properties, and complete amino acid sequence of human secretory leukocyte protease inhibitor, a potent inhibitor of leukocyte elastase. *Proc. Natl. Acad. Sci. USA* 83: 6692–6696.
16. Ashcroft, G. S., K. Lei, W. Jin, G. Longenecker, A. B. Kulkarni, T. Greenwell-Wild, H. Hale-Donze, G. McGrady, X. Y. Song, and S. M. Wahl. 2000. Secretory leukocyte protease inhibitor mediates non-redundant functions necessary for normal wound healing. *Nat. Med.* 6: 1147–1153.

17. Zhu, J., C. Nathan, W. Jin, D. Sim, G. S. Ashcroft, S. M. Wahl, L. Lacomis, H. Erdjument-Bromage, P. Tempst, C. D. Wright, and A. Ding. 2002. Conversion of proepithelin to epithelins: roles of SLPI and elastase in host defense and wound repair. *Cell* 111: 867–878.
18. Hiemstra, P. S., R. J. Maassen, J. Stolk, R. Heinzel-Wieland, G. J. Steffens, and J. H. Dijkman. 1996. Antibacterial activity of antileukoprotease. *Infect. Immun.* 64: 4520–4524.
19. McNeely, T. B., D. C. Shugars, M. Rosendahl, C. Tucker, S. P. Eisenberg, and S. M. Wahl. 1997. Inhibition of human immunodeficiency virus type 1 infectivity by secretory leukocyte protease inhibitor occurs prior to viral reverse transcription. *Blood* 90: 1141–1149.
20. Tomee, J. F., P. S. Hiemstra, R. Heinzel-Wieland, and H. F. Kauffman. 1997. Antileukoprotease: an endogenous protein in the innate mucosal defense against fungi. *J. Infect. Dis.* 176: 740–747.
21. Simpson, A. J., A. L. Maxwell, J. R. Govan, C. Haslett, and J. M. Sallenave. 1999. Elafin (elastase-specific inhibitor) has anti-microbial activity against Gram-positive and Gram-negative respiratory pathogens. *FEBS Lett.* 452: 309–313.
22. Yenugu, S., R. T. Richardson, P. Sivashanmugam, Z. Wang, M. G. O'Rand, F. S. French, and S. H. Hall. 2004. Antimicrobial activity of human EPPIN, an androgen-regulated, sperm-bound protein with a whey acidic protein motif. *Biol. Reprod.* 71: 1484–1490.
23. Jin, F. Y., C. Nathan, D. Radzioch, and A. Ding. 1997. Secretory leukocyte protease inhibitor: a macrophage product induced by and antagonistic to bacterial lipopolysaccharide. *Cell* 88: 417–426.
24. Taggart, C. C., S. A. Cryan, S. Weldon, A. Gibbons, C. M. Greene, E. Kelly, T. B. Low, S. J. O'Neill, and N. G. McElvaney. 2005. Secretory leucoprotease inhibitor binds to NF-κB binding sites in monocytes and inhibits p65 binding. *J. Exp. Med.* 202: 1659–1668.
25. Taggart, C. C., C. M. Greene, N. G. McElvaney, and S. O'Neill. 2002. Secretory leucoprotease inhibitor prevents lipopolysaccharide-induced IκBα degradation without affecting phosphorylation or ubiquitination. *J. Biol. Chem.* 277: 33648–33653.
26. Nakamura, A., Y. Mori, K. Hagiwara, T. Suzuki, T. Sakakibara, T. Kikuchi, T. Igarashi, M. Ebina, T. Abe, J. Miyazaki, et al. 2003. Increased susceptibility to LPS-induced endotoxin shock in secretory leukoprotease inhibitor (SLPI)-deficient mice. *J. Exp. Med.* 197: 669–674.
27. Ding, A., H. Yu, J. Yang, S. Shi, and S. Ehrt. 2005. Induction of macrophage-derived SLPI by *Mycobacterium tuberculosis* depends on TLR2 but not MyD88. *Immunology* 116: 381–389.
28. Doi, T., H. Yamada, T. Yajima, W. Wajjwalku, T. Hara, and Y. Yoshikai. 2007. H2–M3-restricted $CD8^+$ T cells induced by peptide-pulsed dendritic cells confer protection against *Mycobacterium tuberculosis*. *J. Immunol.* 178: 3806–3813.
29. deMello, D. E., S. Mahmoud, P. J. Padfield, and J. W. Hoffmann. 2000. Generation of an immortal differentiated lung type-II epithelial cell line from the adult H-$2K^b$tsA58 transgenic mouse. *In Vitro Cell. Dev. Biol. Anim.* 36: 374–382.
30. Aoki, K., S. Matsumoto, Y. Hirayama, T. Wada, Y. Ozeki, M. Niki, P. Domenech, K. Umemori, S. Yamamoto, A. Mineda, et al. 2004. Extracellular mycobacterial DNA-binding protein 1 participates in mycobacterium-lung epithelial cell interaction through hyaluronic acid. *J. Biol. Chem.* 279: 39798–39806.
31. Loh, B., C. Grant, and R. E. Hancock. 1984. Use of the fluorescent probe 1-*N*-phenylnaphthylamine to study the interactions of aminoglycoside antibiotics with the outer membrane of *Pseudomonas aeruginosa*. *Antimicrob. Agents Chemother.* 26: 546–551.
32. Jat, P. S., M. D. Noble, P. Ataliotis, Y. Tanaka, N. Yannoutsos, L. Larsen, and D. Kioussis. 1991. Direct derivation of conditionally immortal cell lines from an H-$2K^b$-tsA58 transgenic mouse. *Proc. Natl. Acad. Sci. USA* 88: 5096–5100.
33. Whitehead, R. H., P. E. VanEeden, M. D. Noble, P. Ataliotis, and P. S. Jat. 1993. Establishment of conditionally immortalized epithelial cell lines from both colon and small intestine of adult H-$2K^b$-tsA58 transgenic mice. *Proc. Natl. Acad. Sci. USA* 90: 587–591.
34. Si-Tahar, M., D. Merlin, S. Sitaraman, and J. L. Madara. 2000. Constitutive and regulated secretion of secretory leukocyte proteinase inhibitor by human intestinal epithelial cells. *Gastroenterology* 118: 1061–1071.
35. Kirchhoff, C., I. Habben, R. Ivell, and N. Krull. 1991. A major human epididymis-specific cDNA encodes a protein with sequence homology to extracellular proteinase inhibitors. *Biol. Reprod.* 45: 350–357.
36. Miyakawa, Y., P. Ratnakar, A. G. Rao, M. L. Costello, O. Mathieu-Costello, R. I. Lehrer, and A. Catanzaro. 1996. In vitro activity of the antimicrobial peptides human and rabbit defensins and porcine leukocyte protegrin against *Mycobacterium tuberculosis*. *Infect. Immun.* 64: 926–932.
37. Zasloff, M. 2002. Antimicrobial peptides of multicellular organisms. *Nature* 415: 389–395.
38. Tanabe, H., X. Qu, C. S. Weeks, J. E. Cummings, S. Kolusheva, K. B. Walsh, R. Jelinek, T. K. Vanderlick, M. E. Selsted, and A. J. Ouellette. 2004. Structure-activity determinants in Paneth cell α-defensins: loss-of-function in mouse cryptdin-4 by charge-reversal at arginine residue positions. *J. Biol. Chem.* 279: 11976–11983.
39. Grutter, M. G., G. Fendrich, R. Huber, and W. Bode. 1988. The 2.5 A X-ray crystal structure of the acid-stable proteinase inhibitor from human mucous secretions analysed in its complex with bovine α-chymotrypsin. *EMBO J.* 7: 345–351.
40. Lin, C. C., and J. Y. Chang. 2006. Pathway of oxidative folding of secretory leucocyte protease inhibitor: an 8-disulfide protein exhibits a unique mechanism of folding. *Biochemistry* 45: 6231–6240.

Enhanced TLR-mediated NF-IL6–dependent gene expression by Trib1 deficiency

Masahiro Yamamoto,[1,3] Satoshi Uematsu,[1] Toru Okamoto,[2] Yoshiharu Matsuura,[2] Shintaro Sato,[4] Himanshu Kumar,[1] Takashi Satoh,[1,4] Tatsuya Saitoh,[1] Kiyoshi Takeda,[3,5] Ken J. Ishii,[4] Osamu Takeuchi,[1,4] Taro Kawai,[1,4] and Shizuo Akira[1,4]

[1]Department of Host Defense and [2]Department of Molecular Virology, Research Institute for Microbial Diseases and [3]Department of Microbiology and Immunology, Graduate School of Medicine, Osaka University, Suita, Osaka 565-0871, Japan
[4]Exploratory Research for Advanced Technology, Japan Science and Technology Corporation, Suita, Osaka, 565-0871, Japan
[5]Department of Embryonic and Genetic Engineering, Medical Institute of Bioregulation, Kyushu University, Higashi-ku, Fukuoka 812-8582, Japan

Toll-like receptors (TLRs) recognize a variety of microbial components and mediate downstream signal transduction pathways that culminate in the activation of nuclear factor κB (NF-κB) and mitogen-activated protein (MAP) kinases. Trib1 is reportedly involved in the regulation of NF-κB and MAP kinases, as well as gene expression in vitro. To clarify the physiological function of Trib1 in TLR-mediated responses, we generated Trib1-deficient mice by gene targeting. Microarray analysis showed that Trib1-deficient macrophages exhibited a dysregulated expression pattern of lipopolysaccharide-inducible genes, whereas TLR-mediated activation of MAP kinases and NF-κB was normal. Trib1 was found to associate with NF-IL6 (also known as CCAAT/enhancer-binding protein β). NF-IL6–deficient cells showed opposite phenotypes to those in Trib1-deficient cells in terms of TLR-mediated responses. Moreover, overexpression of Trib1 inhibited NF-IL6–dependent gene expression by down-regulating NF-IL6 protein expression. In contrast, Trib1-deficient cells exhibited augmented NF-IL6 DNA-binding activities with increased amounts of NF-IL6 proteins. These results demonstrate that Trib1 is a negative regulator of NF-IL6 protein expression and modulates NF-IL6–dependent gene expression in TLR-mediated signaling.

CORRESPONDENCE
Shizuo Akira:
sakira@biken.osaka-u.ac.jp

Abbreviations used: 24p3, lipocalin-2; BLP, bacterial lipoprotein; C/EBP, CCAAT/enhancer-binding protein; Jnk, c-Jun N-terminal kinase; MALP-2, macrophage-activating lipopeptide-2; MAP, mitogen-activated protein; mPGES, prostaglandin E synthase; TLR, Toll-like receptor.

Innate immunity is promptly activated after the invasion of microbes through recognition of pathogen-associated molecular patterns by pattern-recognition receptors, including Toll-like receptors (TLRs) (1). The recognition of microbial components by TLRs effectively stimulates host immune responses such as proinflammatory cytokine production, cellular proliferation, and up-regulation of co-stimulatory molecules, accompanied by the activation of NF-κB and mitogen-activated protein (MAP) kinases (2, 3). Although the inhibitory protein IκB family members sequester NF-κB in the cytoplasm of unstimulated cells, TLR-dependent IκB phosphorylation by the IκB kinase complex and degradation by the ubiquitin–proteasome pathway permit translocation of NF-κB to the nucleus (4). MAP kinases such as c-Jun N-terminal kinase (Jnk) and p38 are also rapidly phosphorylated and activated by upstream kinases in response to TLR stimulation (5). Moreover, TLR-mediated activity of NF-κB and MAP kinases is shown to be regulated at multiple steps regarding the strength and the duration of the activation (6).

Recent extensive experiments have identified a variety of modulators that have positive and negative effects on the activation of NF-κB and MAP kinases, including a family of serine/threonine kinase-like proteins called Trib (7). Trib consists of three family members: Trib1 (also known as c8fw, GIG2, or SKIP1), Trib2 (also known as c5fw), and Trib3 (also known as NIPK, SINK, or SKIP3) (7–12). Trib3 has been shown to interact with the p65 subunit of NF-κB and to inhibit NF-κB–dependent gene expression in vitro (11). In terms of MAP kinases, Trib1, Trib2, and Trib3 reportedly bind to Jnk and p38, and affect the activity of MAP kinases and IL-8 production in response to PMA or

The online version of this article contains supplemental material.

JEM © The Rockefeller University Press $30.00
Vol. 204, No. 9, September 3, 2007 2233-2239 www.jem.org/cgi/doi/10.1084/jem.20070183

TLR ligands/IL-1 (12). However, whether Trib family members regulate TLR-mediated signaling pathways under physiological conditions is still unknown.

In this study, we generated Trib1-deficient mice by gene targeting and analyzed TLR-mediated responses. Although the activation of NF-κB and MAP kinases in response to LPS was comparable between wild-type and Trib1-deficient cells, microarray analysis revealed that a subset of LPS-inducible genes was dysregulated in Trib1-deficient cells. Subsequent yeast two-hybrid analysis identified the CCAAT/enhancer-binding protein (C/EBP) family member NF-IL6 (also known as C/EBPβ) as a binding partner of Trib1, and phenotypes found in NF-IL6–deficient cells were opposite to those observed in Trib1-deficient cells. Moreover, overexpression of Trib1 inhibited NF-IL6–mediated gene expression and reduced amounts of NF-IL6 proteins. Inversely, NF-IL6 DNA-binding activity and LPS-inducible NF-IL6–target gene expression were up-regulated in Trib1-deficient cells, in which amounts of NF-IL6 proteins were increased. These results demonstrate that Trib1 plays an important role in NF-IL6–dependent gene expression in the TLR-mediated signaling pathways.

RESULTS

Comprehensive gene expression analysis in Trib1-deficient macrophages

To assess the physiological function of Trib1 in TLR-mediated immune responses, we performed a microarray analysis to compare gene expression profiles between wild-type and Trib1-deficient macrophages in response to LPS (Fig. 1 A and Fig. S1, available at http://www.jem.org/cgi/content/full/jem.20070183/DC1). Out of 45,102 transcripts, we first defined the genes induced more than twofold after LPS stimulation in wild-type cells as "LPS-inducible genes" and identified 790 of them (Table S1). We next compared the LPS-inducible genes in wild-type and Trib1-deficient macrophages after LPS stimulation and found 59, 703, and 28 genes as up-regulated, similarly expressed, and down-regulated in Trib1-deficient cells, respectively (Table S1).

Among the up-regulated genes, several were subsequently tested by Northern blotting to confirm the accuracy. LPS-induced expression of prostaglandin E synthase (mPGES), lipocalin-2 (24p3), arginase type II, and plasminogen activator inhibitor type II, which were highly up-regulated in the microarray analysis (Table S1), was indeed enhanced in Trib1-deficient macrophages (Fig. 1 B). Furthermore, in contrast to proinflammatory cytokines such as TNF-α and IL-6, which were similarly expressed between wild-type and Trib1-deficient cells in response not only to LPS but also to other TLR ligands, IL-12 p40 was down-regulated in Trib1-deficient cells compared with wild-type cells (Fig. 1 C; Fig. S2, A–C, available at http://www.jem.org/cgi/content/full/jem.20070183/DC1; and Table S1). Thus, the comprehensive microarray analysis revealed that a subset of LPS-inducible genes is dysregulated in Trib1-deficient cells.

Previous in vitro studies demonstrate that human Trib family members modulate activation of MAP kinases and

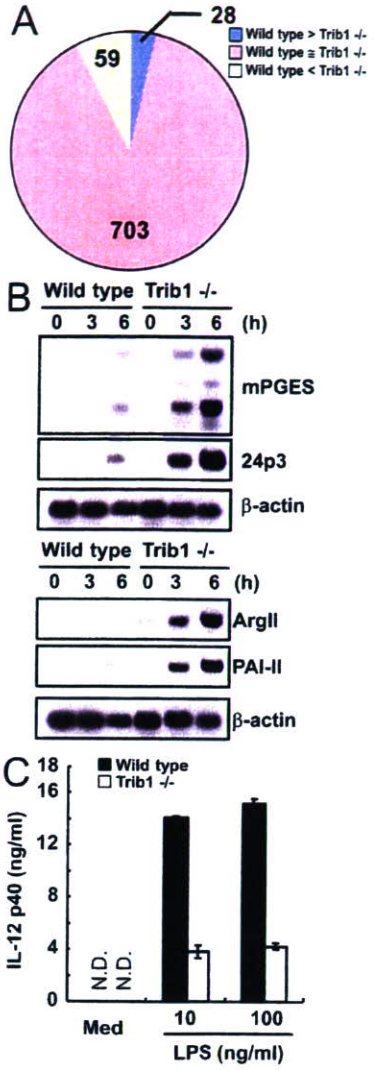

Figure 1. Dysregulation of a subset of LPS-inducible genes in Trib1-deficient cells. (A) Summary of DNA chip microarray analysis. 790 LPS-inducible genes were divided into up-regulated (yellow), similarly expressed (pink), and down-regulated (blue) groups, with the indicated amounts of each. (B) Peritoneal macrophages from wild-type or Trib1-deficient mice were stimulated with 10 ng/ml LPS for the indicated periods. Total RNA (10 μg) was extracted and subjected to Northern blot analysis for the expression of the indicated probes. (C) Peritoneal macrophages from wild-type and Trib1-deficient mice were cultured with the indicated concentrations of LPS in the presence of 30 ng/ml IFN-γ for 24 h. Concentrations of IL-12 p40 in the culture supernatants were measured by ELISA. Indicated values are means ± SD of triplicates. Data are representative of three (B) or two (C) independent experiments. N.D., not detected.

NF-κB (7–12). Both wild-type and Trib1-deficient cells showed similar levels and time courses of phosphorylation of p38, Jnk and extracellular signal-regulated kinase, and IκBα degradation (Fig. S2 D), indicating that the dysregulated

expression of LPS-inducible genes in Trib1-deficient cells might be the independent of activation of NF-κB and MAP kinases.

Interaction of Trib1 with NF-IL6

To explore signaling aspects of Trib1 deficiency other than NF-κB and MAP kinases, we performed a yeast-two-hybrid screen with the full length of human Trib1 as bait to identify a binding partner of Trib1 and identified several clones as being positive. Sequence analysis subsequently revealed that three clones encoded the N-terminal portion of a member of the C/EBP NF-IL6 (unpublished data). We initially tested the interaction of Trib1 and NF-IL6 in yeasts. AH109 cells were transformed with a plasmid encoding the full length of Trib1 together with a plasmid encoding the N-terminal portion of NF-IL6 obtained by the screening (Fig. 2 A). We next examined the interaction in mammalian cells using immunoprecipitation experiments. HEK293 cells were transiently transfected with a plasmid encoding the full length of mouse Trib1 together with a plasmid encoding the full length of mouse NF-IL6. Myc-tagged NF-IL6 was coimmunoprecipitated with Flag-Trib1 (Fig. 2 B), showing the interaction of Trib1 and NF-IL6 in mammalian cells.

TLR-mediated immune responses in NF-IL6–deficient macrophages

An in vitro study showing the interaction of Trib1 and NF-IL6 prompted us to examine the TLR-mediated immune responses in NF-IL6–deficient cells, because LPS-induced expression of mPGES is shown to depend on NF-IL6 (13). We initially analyzed the expression pattern of genes affected by the loss of Trib1 in NF-IL6–deficient macrophages by Northern blotting. LPS-induced expression of 24p3, plasminogen activator inhibitor type II, and arginase type II, as well as mPGES, was profoundly defective in NF-IL6–deficient cells (Fig. 2 C). We next tested IL-12 p40 production by ELISA. As previously reported, IL-12 p40 production by LPS stimulation was increased in a dose-dependent fashion in NF-IL6–deficient cells compared with control cells (Fig. 2 D) (14). In addition, the production in response to bacterial lipoprotein (BLP), macrophage-activating lipopeptide–2 (MALP-2), or CpG DNA was also augmented in

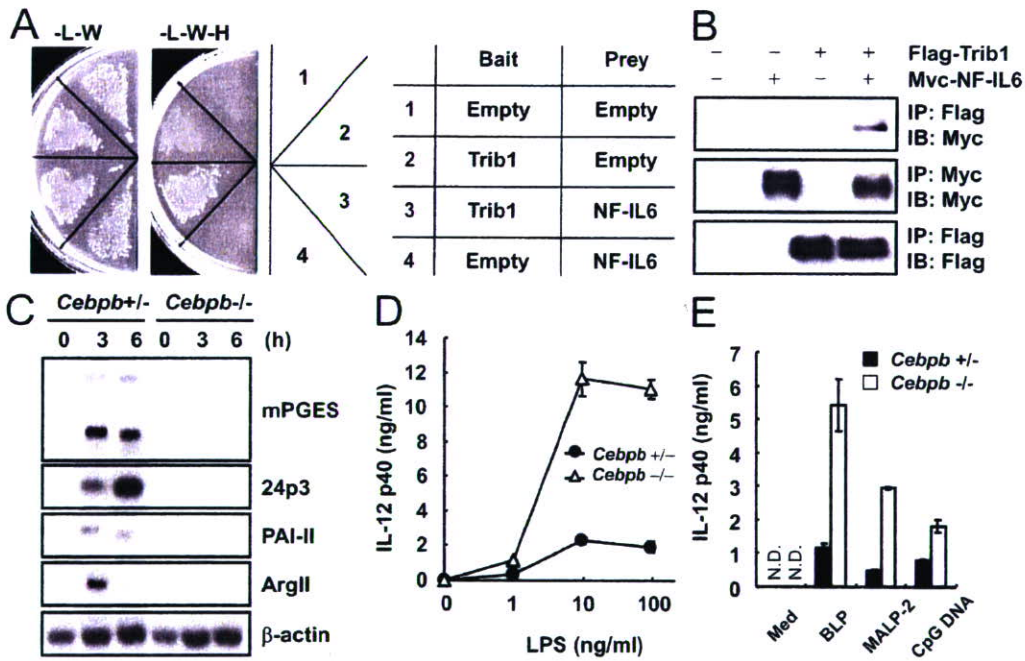

Figure 2. Association of Trib1 with NF-IL6 and TLR-mediated responses in NF-IL6–deficient macrophages. (A) Plasmids expressing human Trib1 fused to the GAL4 DNA-binding domain or an empty vector were cotransfected with a plasmid expressing NF-IL6 fused to GAL4 transactivation domain or an empty vector. Interactions were detected by the ability of cells to grow on medium lacking tryptophan, leucin, and histidine (-L-W-H). The growth of cells on a plate lacking tryptophan and leucine (-L-W) is indicative of the efficiency of the transfection. (B) Lysates of HEK293 cells transiently cotransfected with 2 μg of Flag-tagged Trib1 and/or 2 μg Myc-tagged NF-IL6 expression vectors were immunoprecipitated with the indicated antibodies. (C) Peritoneal macrophages from wild-type or NF-IL6–deficient mice were stimulated with 10 ng/ml LPS for the indicated periods. Total RNA (10 μg) was extracted and subjected to Northern blot analysis for expression of the indicated probes. (D and E) Peritoneal macrophages from wild-type and NF-IL6–deficient mice were cultured with the indicated concentrations of LPS (D) or with 100 ng/ml BLP, 30 ng/ml MALP-2, or 1 μM, CpG DNA (E) in the presence of 30 ng/ml IFN-γ for 24 h. Concentrations of IL-12 p40 in the culture supernatants were measured by ELISA. Indicated values are means ± SD of triplicates. Data are representative of three (B) and two (C–E) separate experiments. N.D., not detected.

NF-IL6–deficient cells (Fig. 2 E). Together, compared with Trib1-deficient cells, converse phenotypes in terms of TLR-mediated immune responses are observed in NF-IL6–deficient cells.

Inhibition of NF-IL6 by Trib1 overexpression

To test whether Trib1 down-regulates NF-IL6–dependent activation, HEK293 cells were transfected with an NF-IL6–dependent luciferase reporter plasmid together with NF-IL6 and various amounts of Trib1 expression vectors (Fig. 3 A). NF-IL6–mediated luciferase activity was diminished by co-expression of Trib1 in a dose-dependent manner. Moreover, RAW264.7 macrophage cells overexpressing Trib1 exhibited reduced expression of mPGES and 24p3 in response to LPS (Fig. S3 A, available at http://www.jem.org/cgi/content/full/jem.20070183/DC1). We next tested NF-IL6 DNA-binding activity by EMSA and observed less NF-IL6 DNA-binding activity in HEK293 cells coexpressing NF-IL6 and Trib1 than in ones transfected with the NF-IL6 vector alone (Fig. 3 B), presumably accounting for the down-regulation of the NF-IL6–dependent gene expression by Trib1. We then examined the effect of Trib1 on the amounts of NF-IL6 proteins by Western blotting. Although the diminution of NF-IL6 by Trib1 was marginal when excess amounts of NF-IL6 were expressed, we found that the transient expression of lower levels of NF-IL6, together with Trib1, resulted in a reduction of NF-IL6 in HEK293 cells (Fig. 3 C). Also, endogenous levels of NF-IL6 proteins in RAW264.7 cells overexpressing Trib1 were markedly less than those in control cells (Fig. 3 D). These results demonstrated that overproduction of Trib1 might negatively regulate NF-IL6 activity in vitro.

Up-regulation of NF-IL6 in Trib1-deficient cells

We next attempted to check the in vivo status of NF-IL6 in Trib1-deficient cells by comparing the NF-IL6 DNA-binding activity in Trib1-deficient macrophages with that in wild-type cells by EMSA. Although LPS-induced NF-κB–DNA complex formation in Trib1-deficient cells was similarly observed, Trib1-deficient cells exhibited elevated levels of C/EBP–DNA complex formation compared with wild-type cells (Fig. 4 A). We further examined whether the C/EBP–DNA complex in Trib1-deficient cells contained NF-IL6 by supershift assay. Addition of anti–NF-IL6 antibody into the C/EBP–DNA complex yielded more supershifted bands in Trib1-deficient cells than in wild-type cells (Fig. 4 B). In addition, the C/EBP–DNA complex was not shifted by the addition of anti-C/EBPδ (also known as NF-IL6β) antibody (Fig. S4 A, available at http://www.jem.org/cgi/content/full/jem.20070183/DC1), suggesting that NF-IL6 DNA-binding activity is augmented in Trib1-deficient cells. We then examined the amounts of NF-IL6 proteins by Western blotting (Fig. 4 C). Compared with wild-type cells, Trib1-deficient cells showed increased levels of NF-IL6 proteins. Finally, we examined NF-IL6 mRNA levels by Northern blotting and observed enhanced expression of NF-IL6 mRNA in Trib1-deficient cells (Fig. 4 D), which is consistent with the autocrine induction of NF-IL6 mRNA

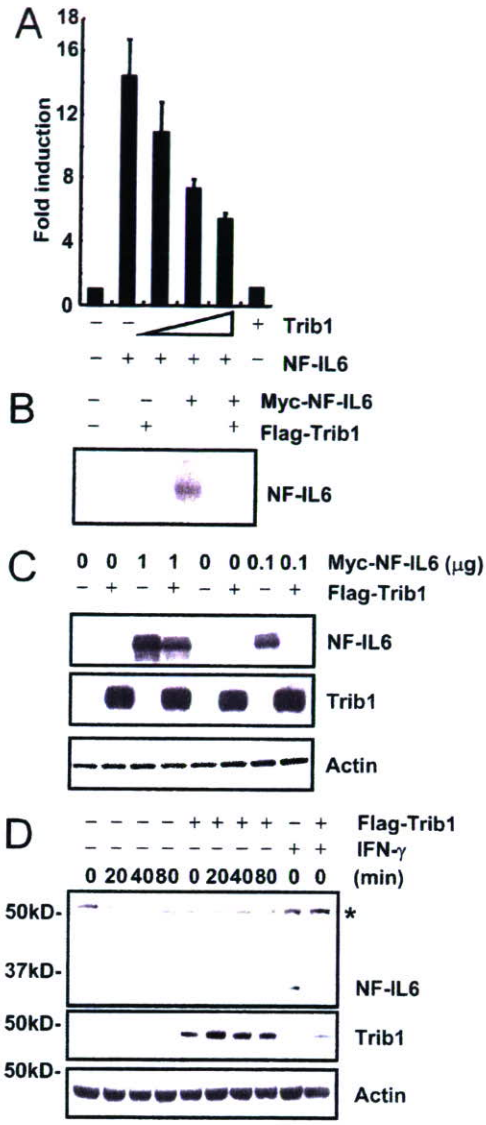

Figure 3. Inhibition of NF-IL6 activity by Trib1 overexpression. (A) HEK293 cells were transfected with an NF-IL6–dependent luciferase reporter together with either Trib1 and/or NF-IL6 expression plasmids. Luciferase activities were expressed as the fold increase over the background shown by lysates prepared from mock-transfected cells. Indicated values are means ± SD of triplicates. (B) HEK293 cells were transfected with 0.1 μg NF-IL6 expression vector together with 4 μg Trib1 expression plasmids. Nuclear extracts were prepared, and C/EBP DNA-binding activity was determined by EMSA using a probe containing the NF-IL6 binding sequence from the mouse 24p3 gene. (C) Lysates of HEK293 cells transiently cotransfected with 2 μg of Flag-tagged Trib1 alone or the indicated amounts of Myc-tagged NF-IL6 expression vectors were immunoblotted with anti-Myc or -Flag for detection of NF-IL6 or Trib1, respectively. (E) RAW 264.7 cells stably transfected with either an empty vector or Flag-Trib1 were stimulated with 10 ng/ml LPS for the indicated periods. The cell lysates were immunoblotted with the indicated antibodies. A protein that cross-reacts with the antibody is indicated (*). Data are representative of three (A and C) and two (B and D), separate experiments.

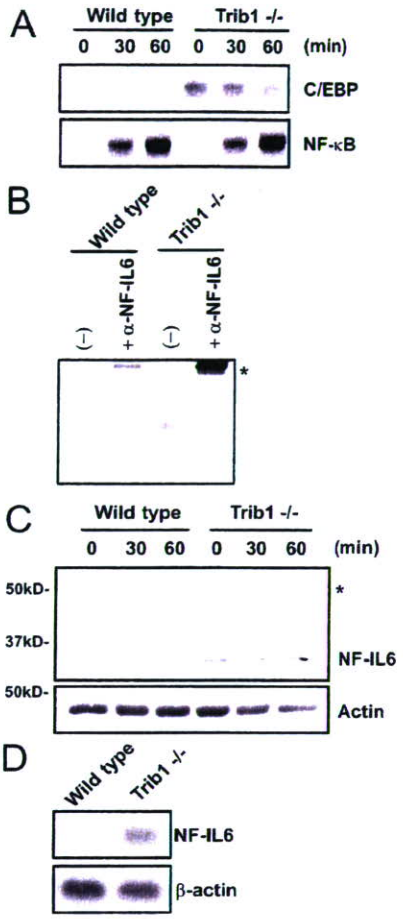

Figure 4. Up-regulation of NF-IL6 activity in Trib1-deficient cells. (A) Peritoneal macrophages from wild-type or Trib1-deficient mice were stimulated with 10 ng/ml LPS for the indicated periods. Nuclear extracts were prepared, and C/EBP DNA-binding activity was determined by EMSA using a C/EBP consensus probe. (B) Nuclear extracts of wild-type and Trib1-deficient unstimulated macrophages were preincubated with anti-NF-IL6, followed by EMSA to determine the C/EBP DNA-binding activity. Supershifted bands are indicated (*). (C) Peritoneal macrophages from wild-type or Trib1-deficient mice were stimulated with 10 ng/ml LPS for the indicated periods and lysed. The cell lysates were immunoblotted with the indicated antibodies. A protein that cross-reacts with the antibody is indicated (*). (D) Total RNA (10 μg) from unstimulated peritoneal macrophages from wild-type or NF-IL6–deficient mice was extracted and subjected to Northern blot analysis for expression of the indicated probes. Data are representative of two (A and B) and three (C and D) separate experiments.

in a previous study (15). Thus, Trib1 may negatively control amounts of NF-IL6 proteins, thereby affecting TLR-mediated NF-IL6–dependent gene induction.

DISCUSSION

In this study, we demonstrate by microarray analysis and biochemical studies that Trib1 is associated with NF-IL6 and negates NF-IL6–dependent gene expression by reducing the amounts of NF-IL6 proteins in the context of TLR-mediated responses. Especially regarding IL-12 p40, although the microarray data showed an almost twofold reduction of the mRNA in Trib1-deficient cells (Table S1), the production was three to four times lower than that in wild-type cells (Fig. 1 C), suggesting translational control of IL-12 p40 by Trib1 in addition to the transcriptional regulation. Moreover, the transcription of the IL-12 p40 gene itself may be affected by not only the amount of NF-IL6 proteins but also the phosphorylation or the isoforms such as liver-enriched activator protein and liver-enriched inhibitory protein (16–18). The molecular mechanisms of how Trib1 deficiency affects IL-12 p40 production on the transcriptional or translational levels through NF-IL6 regulation need to be carefully studied in the future.

The name Trib is originally derived from the *Drosophila* mutant strain *tribbles*, in which the *Drosophila* tribbles protein negatively regulates the level of *Drosophila* C/EBP *slbo* protein and C/EBP-dependent developmental responses such as border cell migration in larvae (19–22). It is also of interest that Trib1-deficient female mice and *Drosophila* in adulthood are both infertile (unpublished data) (18). In mammals, other Trib family members such as Trib2 and Trib3 have recently been shown to be involved in C/EBP-dependent responses (23, 24). Mice transferred with bone marrow cells, in which Trib2 is retrovirally overexpressed, display acute myelogenous leukemia–like disease with reduced activities and amounts of C/EBPα (23). In addition, ectopic expression of Trib3 inhibits C/EBP-homologous protein–induced ER stress–mediated apoptosis (24). Thus, the function of tribbles to inhibit C/EBP activities by controlling the amounts appears to be conserved throughout evolution.

Given the up-regulation of the mRNA in Trib1-deficient cells (Fig. 4 D), the reduction of NF-IL6 in Trib1-overexpressing cells (Fig. 3 C), the auto-regulation of NF-IL6 by itself (15), and the degradation of C/EBPα by Trib2 (23) and slbo by tribbles (22), the loss of Trib1 might primarily result in impaired degradation of NF-IL6 and, subsequently, in excessive accumulation of NF-IL6 via the autoregulation in Trib1-deficient cells.

In this study, we focused on the involvement of Trib1 in TLR-mediated NF-IL6–dependent gene expression. However, given that the levels of NF-IL6 proteins were increased in Trib1-deficient cells, it is reasonable to propose that other non–TLR-related NF-IL6–dependent responses might be enhanced in Trib1-deficient mice. Moreover, Trib3 is also shown to be involved in insulin-mediated Akt/PKB activation in the liver by mechanisms apparently unrelated to C/EBP, suggesting that Trib family members possibly function in a C/EBP-independent fashion (25–27). Future studies using mice lacking other Trib family members, as well as Trib1, may help to unravel the nature of mammalian tribbles in wider points of view.

MATERIALS AND METHODS

Generation of Trib1-deficient mice. A genomic DNA containing the *Trib1* gene was isolated from the 129/SV mouse genomic library and characterized by restriction enzyme mapping and sequencing analysis. The gene encoding mouse Trib1 consists of three exons. The targeting vector was constructed by replacing a 0.4-kb fragment encoding the second exon of the

Trib1 gene with a neomycin resistance gene cassette (*neo*) (Fig. S1 A). The targeting vector was transfected into embryonic stem cells (E14.1). G418 and gancyclovir doubly resistant colonies were selected and screened by PCR and Southern blot analysis (Fig. S1 B). Homologous recombinants were microinjected into C57BL/6 female mice, and heterozygous F1 progenies were intercrossed to obtain *Trib1*$^{-/-}$ mice. We interbred the heterozygous mice to produce offspring carrying a null mutation of the gene encoding Trib1. Trib1-deficient mice were born at the expected Mendelian ratio and showed a slight growth retardation with reduced body weight until 2–3 wk after birth (unpublished data). Trib1-deficient that mice survived for >6 wk were analyzed in this study. To confirm the disruption of the gene encoding Trib1, we analyzed total RNA from wild-type and Trib1-deficient peritoneal macrophages by Northern blotting and found no transcripts for Trib1 in Trib1-deficient cells (Fig. S1 C). All animal experiments were conducted with the approval of the Animal Research Committee of the Research Institute for Microbial Diseases at Osaka University.

Reagents, cells, and mice. LPS (a TLR4 ligand) from *Salmonella minnesota* Re 595 and anti-Flag were purchased from Sigma-Aldrich. BLP (TLR1/TLR2), MALP-2 (TLR2/TLR6), and CpG oligodeoxynucleotides (TLR9) were prepared as previously described (28). Antiphosphorylated extracellular signal-regulated kinase, Jnk, and p38 antibodies were purchased from Cell Signaling. Anti–NF-IL6 (C/EBPβ), C/EBPδ, actin, IκBα, and Myc-probe were obtained from Santa Cruz Biotechnology, Inc. NF-IL6–deficient mice were as previously described (29). Epitope-tagged Trib1 fragments were generated by PCR using cDNA from LPS-stimulated mouse peritoneal macrophages as the template and cloned into pcDNA3 expression vectors, according to the manufacturer's instructions (Invitrogen).

Measurement of proinflammatory cytokine concentrations. Peritoneal macrophages were collected from peritoneal cavities 96 h after thioglycollate injection and cultured in 96-well plates (10^5 cells per well) with the indicated concentrations of the indicated ligands for 24 h, as shown in the figures. Concentrations of TNF-α, IL-6, and IL-12 p40 in the culture supernatant were measured by ELISA, according to manufacturer's instructions (TNF-α and IL-12 p40, Genzyme; IL-6, R&D Systems).

Luciferase reporter assay. The NF-IL6–dependent reporter plasmids were constructed by inserting the promoter regions (−1200 to +53) of the mouse 24p3 gene amplified by PCR into the pGL3 reporter plasmid. The reporter plasmids were transiently cotransfected into HEK293 with the control *Renilla* luciferase expression vectors using a reagent (Lipofectamine 2000; Invitrogen). Luciferase activities of total cell lysates were measured using the Dual-Luciferase Reporter Assay System (Promega), as previously described (28).

Yeast two-hybrid analysis. Yeast two-hybrid screening was performed as described for the Matchmaker two-hybrid system 3 (CLONTECH Laboratories, Inc.). For construction of the bait plasmid, the full length of human Trib1 was cloned in frame into the GAL4 DNA-binding domain of pG-BKT7. Yeast strain AH109 was transformed with the bait plasmid plus the human lung Matchmaker cDNA library. After screening of 10^6 clones, positive clones were picked, and the pACT2 library plasmids were recovered from individual clones and expanded in *Escherichia coli*. The insert cDNA was sequenced and characterized with the BLAST program (National Center for Biotechnology Information).

Microarray analysis. Peritoneal macrophages from wild-type or Trib1-deficient mice were left untreated or were treated for 4 h with 10 ng/ml LPS in the presence of 30 ng/ml IFN-γ. The cDNA was synthesized and hybridized to Murine Genome 430 2.0 microarray chips (Affymetrix), according to the manufacturer's instructions. Hybridized chips were stained and washed and were scanned with a scanner (GeneArray; Affymetrix). Microarray Suite software (version 5.0; Affymetrix) was used for data analysis. Microarray data have been deposited in the Gene Expression Omnibus under accession no. GSE8788.

Western blot analysis and immunoprecipitation. Peritoneal macrophages were stimulated with the indicated ligands for the indicated periods, as shown in the figures. The cells were lysed in a lysis buffer (1% Nonidet P-40, 150 mM NaCl, 20 mM Tris-Cl [pH 7.5], 5 mM EDTA) and a protease inhibitor cocktail (Roche). The cell lysates were separated by SDS-PAGE and transferred to polyvinylidene difluoride membranes. For immunoprecipitation, cell lysates were precleared with protein G–sepharose (GE Healthcare) for 2 h and incubated with protein G–sepharose containing 1 μg of the antibodies indicated in the figures for 12 h, with rotation at 4°C. The immunoprecipitants were washed four times with lysis buffer, eluted by boiling with Laemmli sample buffer, and subjected to Western blot analysis using the indicated antibodies, as previously described (28).

EMSA and supershift assay. 2×10^6 peritoneal macrophages were stimulated with the indicated stimulants for the indicated periods, as shown in the figures. 2×10^6 HEK293 cells were transfected with 0.1 μg Myc–NF-IL6 and/or 4 μg Flag-Trib1 expression vectors. Nuclear extracts were purified from cells and incubated with a probe containing a consensus C/EBP DNA-binding sequence (5′-TGCAGATTGCGCAATCTGCA-3′; Fig. 4, A and B) or mouse 24p3 NF-IL6 binding sequence (sense, 5′-CTTCCTGTTGCTCAACCTTGCA-3′;antisense,5′-TGCAAGGTTGAGCAACAGGAAG-3′; Fig. 3 B), electrophoresed, and visualized by autoradiography, as previously described (28, 30). When the supershift assay was performed, nuclear extracts were mixed with the supershift-grade antibodies indicated in the figures before the incubation with the probes for 1 h on ice.

Online supplemental material. Fig. S1 showed our strategy for the targeted disruption of the mouse *Trib1* gene. Fig. S2 showed the status of proinflammatory cytokine production in response to various TLR ligands and LPS-induced activation of MAP kinases and IκB degradation. Fig. S3 showed decreased expression of NF-IL6–dependent gene in Trib1-overexpressing cells. Fig. S4 showed that the C/EBP-DNA complex in Trib1-deficient cells contained NF-IL6, but not C/EBPδ. Table S1 provides a complete list of the LPS-inducible genes studied. Online supplemental material is available at http://www.jem.org/cgi/content/full/jem.20070183/DC1.

We thank M. Hashimoto for excellent secretarial assistance, and N. Okita, N. Iwami, N. Fukuda, and M. Morita for technical assistance.

This study was supported by the Special Coordination Funds, the Ministry of Education, Culture, Sports, Science and Technology, research fellowships from the Japan Society for the Promotion of Science for Young Scientists, the Uehara Memorial Foundation, the Naito Foundation, the Institute of Physical and Chemical Research Junior Research Associate program, and the National Institutes of Health (grant AI070167).

The authors have no conflicting financial interests.

Submitted: 24 January 2007
Accepted: 26 July 2007

REFERENCES

1. Akira, S., S. Uematsu, and O. Takeuchi. 2006. Pathogen recognition and innate immunity. *Cell.* 124:783–801.
2. Beutler, B. 2004. Inferences, questions and possibilities in Toll-like receptor signalling. *Nature.* 430:257–263.
3. Kopp, E., and R. Medzhitov. 2003. Recognition of microbial infection by Toll-like receptors. *Curr. Opin. Immunol.* 15:396–401.
4. Hayden, M.S., and S. Ghosh. 2004. Signaling to NF-κB. *Genes Dev.* 18:2195–2224.
5. Zhang, Y.L., and C. Dong. 2005. MAP kinases in immune responses. *Cell. Mol. Immunol.* 2:20–27.
6. Miggin, S.M., and L.A. O'Neill. 2006. New insights into the regulation of TLR signaling. *J. Leukoc. Biol.* 80:220–226.
7. Hegedus, Z., A. Czibula, and E. Kiss-Toth. 2007. Tribbles: A family of kinase-like proteins with potent signalling regulatory function. *Cell. Signal.* 19:238–250.
8. Kiss-Toth, E., S.M. Bagstaff, H.Y. Sung, V. Jozsa, C. Dempsey, J.C. Caunt, K.M. Oxley, D.H. Wyllie, T. Polgar, M. Harte et al. 2004.

Human tribbles, a protein family controlling mitogen-activated protein kinase cascades. *J. Biol. Chem.* 279:42703–42708.
9. Wilkin, F., N. Suarez-Huerta, B. Robaye, J. Peetermans, F. Libert, J.E. Dumont, and C. Maenhaut. 1997. Characterization of a phosphoprotein whose mRNA is regulated by the mitogenic pathways in dog thyroid cells *Eur. Eur. J. Biochem.* 248:660–668.
10. Mayumi-Matsuda, K., S. Kojima, H. Suzuki, and T. Sakata. 1999. Identification of a novel kinase-like gene induced during neuronal cell death. *Biochem. Biophys. Res. Commun.* 258:260–264.
11. Wu, M., L.G. Xu, Z. Zhai, and H.B. Shu. 2003. SINK is a p65-interacting negative regulator of NF-κB-dependent transcription. *J. Biol. Chem.* 278:27072–27079.
12. Kiss-Toth, E., D.H. Wyllie, K. Holland, L. Marsden, V. Jozsa, K.M. Oxley, T. Polgar, E.E. Qwarnstrom, and S.K. Dower. 2006. Functional mapping and identification of novel regulators for the Toll/Interleukin-1 signalling network by transcription expression cloning. *Cell. Signal.* 18:202–214.
13. Uematsu, S., M. Matsumoto, K. Takeda, and S. Akira. 2002. Lipopolysaccharide-dependent prostaglandin E(2) production is regulated by the glutathione-dependent prostaglandin E(2) synthase gene induced by the Toll-like receptor 4/MyD88/NF-IL6 pathway. *J. Immunol.* 168:5811–5816.
14. Gorgoni, B., D. Maritano, P. Marthyn, M. Righi, and V. Poli. 2002. C/EBPβ gene inactivation causes both impaired and enhanced gene expression and inverse regulation of IL-12 p40 and p35 mRNAs in macrophages. *J. Immunol.* 168:4055–4062.
15. Ramji, D.P., and P. Foka. 2002. CCAAT/enhancer-binding proteins: structure, function and regulation. *Biochem. J.* 365:561–575.
16. Plevy, S.E., J.H. Gemberling, S. Hsu, A.J. Dorner, and S.T. Smale. 1997. Multiple control elements mediate activation of the murine and human interleukin 12 p40 promoters: evidence of functional synergy between C/EBP and Rel proteins. *Mol. Cell. Biol.* 17:4572–4588.
17. Zhu, C., K. Gagnidze, J.H. Gemberling, and S.E. Plevy. 2001. Characterization of an activation protein-1-binding site in the murine interleukin-12 p40 promoter. Demonstration of novel functional elements by a reductionist approach. *J. Biol. Chem.* 276:18519–18528.
18. Bradley, M.N., L. Zhou, and S.T. Smale. 2003. C/EBPβ regulation in lipopolysaccharide-stimulated macrophages. *Mol. Cell. Biol.* 23:4841–4858.
19. Seher, T.C., and M. Leptin. 2000. Tribbles, a cell-cycle brake that coordinates proliferation and morphogenesis during *Drosophila* gastrulation. *Curr. Biol.* 10:623–629.
20. Mata, J., S. Curado, A. Ephrussi, and P. Rorth. 2000. Tribbles coordinates mitosis and morphogenesis in *Drosophila* by regulating string/CDC25 proteolysis. *Cell.* 101:511–522.
21. Grosshans, J., and E. Wieschaus. 2000. A genetic link between morphogenesis and cell division during formation of the ventral furrow in *Drosophila*. *Cell.* 101:523–531.
22. Rorth, P., K. Szabo, and G. Texido. 2000. The level of C/EBP protein is critical for cell migration during *Drosophila* oogenesis and is tightly controlled by regulated degradation. *Mol. Cell.* 6:23–30.
23. Keeshan, K., Y. He, B.J. Wouters, O. Shestova, L. Xu, H. Sai, C.G. Rodriguez, I. Maillard, J.W. Tobias, P. Valk, et al. 2006. Tribbles homolog 2 inactivates C/EBPα and causes acute myelogenous leukemia. *Cancer Cell.* 10:401–411.
24. Ohoka, N., S. Yoshii, T. Hattori, K. Onozaki, and H. Hayashi. 2005. TRB3, a novel ER stress-inducible gene, is induced via ATF4-CHOP pathway and is involved in cell death. *EMBO J.* 24:1243–1255.
25. Du, K., S. Herzig, R.N. Kulkarni, and M. Montminy. 2003. TRB3: a tribbles homolog that inhibits Akt/PKB activation by insulin in liver. *Science.* 300:1574–1577.
26. Koo, S.H., H. Satoh, S. Herzig, C.H. Lee, S. Hedrick, R. Kulkarni, R.M. Evans, J. Olefsky, and M. Montminy. 2004. PGC-1 promotes insulin resistance in liver through PPAR-alpha-dependent induction of TRB-3. *Nat. Med.* 10:530–534.
27. Qi, L., J.E. Heredia, J.Y. Altarejos, R. Screaton, N. Goebel, S. Niessen, I.X. Macleod, C.W. Liew, R.N. Kulkarni, J. Bain, et al. 2006. TRB3 links the E3 ubiquitin ligase COP1 to lipid metabolism. *Science.* 312:1763–1766.
28. Yamamoto, M., T. Okamoto, K. Takeda, S. Sato, H. Sanjo, S. Uematsu, T. Saitoh, N. Yamamoto, H. Sakurai, K.J. Ishii, et al. 2006. Key function for the Ubc13 E2 ubiquitin-conjugating enzyme in immune receptor signaling. *Nat. Immunol.* 7:962–970.
29. Tanaka, T., S. Akira, K. Yoshida, M. Umemoto, Y. Yoneda, N. Shirafuji, H. Fujiwara, S. Suematsu, N. Yoshida, and T. Kishimoto. 1995. Targeted disruption of the NF-IL6 gene discloses its essential role in bacteria killing and tumor cytotoxicity by macrophages. *Cell.* 80:353–361.
30. Shen, F., Z. Hu, J. Goswami, and S.L. Gaffen. 2006. Identification of common transcriptional regulatory elements in interleukin-17 target genes. *J. Biol. Chem.* 281:24138–24148.

FULL PAPER *Laboratory Animal Science*

Comparison of Estrogen Responsive Genes in the Mouse Uterus, Vagina and Mammary Gland

Atsuko SUZUKI[1,2,3], Hiroshi URUSHITANI[2,3], Hajime WATANABE[2,3], Tomomi SATO[5], Taisen IGUCHI[2,3], Tomohiro KOBAYASHI[6] and Yasuhiko OHTA[3,4]*

[1]*The United Graduate School of Veterinary Science, Yamaguchi University, 1677–1 Yoshida 753–8515,* [2]*Okazaki Institute for Integrative Bioscience, National Institute for Basic Biology, National Institutes of Natural Sciences, 5–1 Higashiyama, Myodaiji, Okazaki 444–8787,* [3]*Core Research for Evolutional Science and Technology, Japan Science and Technology, Kawaguchi,* [4]*Laboratory of Experimental Animals, Department of Veterinary Medicine, Faculty of Agriculture, Tottori University, Koyama 680–8553,* [5]*Graduate School of Integrated Science, Yokohama City University, 22–2 Seto, Kanazawa-ku, Yokohama 236–0027 and* [6]*Depertment of Pharmacology, GlaxsoSmithKline K.K., 43 Wadai, Tukuba, Ibaraki 300–4247, Japan*

(Received 18 December 2006/Accepted 14 March 2007)

ABSTRACT. Female reproductive organs are mainly regulated by estrogen and progesterone. Specifically, the uterus, vagina and mammary gland show organ-specific mitosis and morphological changes during proliferative events, such as estrous cycle, gestation and lactation. The mechanism underlying these organ-specific estrogen-dependent events is still unknown. We examined, therefore, global gene expression in the mature uterus, vagina and mammary gland of ovariectomized adult mice 6 hr after an injection of 5 μg/kg 17β-estradiol (E_2) using a microarray method in order to identify primary E_2-responsive genes. Half of the E_2 up-regulated genes in the uterus were similar to those in the vagina. E_2 up-regulated the expression of *Insulin-like growth factor 1 (Igf-1)* genes in the uterus and vagina. In the vagina, E_2 up-regulated the expression of IGF binding proteins (*Igfbp2* and *Igfbp5*). In the mammary gland, unlike the uterus and vagina, no gene showed altered expression 6 hr after the E_2 exposure. These results suggest that expression of *Igf-1* and morphogenesis genes is regulated by E_2 in an organ-specific manner, and it is supported by the results of BrdU labeling showing E_2-induced mitosis in the uterus and vagina except the mammary gland. The differences in organ specificity in response to E_2 may be attributed by differences in gene expression regulated by E_2 in female reproductive organs. The candidate estrogen-responsive genes in the uterus and vagina identified by profiling provide an important foundation understanding functional mechanisms of estrogen regulating morphogenesis and maintenance of each reproductive organ.

KEY WORDS: estrogen responsive genes, microarray, tissue specificity.

J. Vet. Med. Sci. 69(7): 725–731, 2007

Female reproductive organs vary their morphology during reproductive events, such as differentiation, development, estrous cycle, gestation and lactation. Estrogen is known to have differential developmental effects widely on the uterus, vagina, mammary gland, bone, liver, thymus and brain as its target organs. Although the proliferation of uterine and vaginal epithelia, and ductal elongation of mammary gland in mice could be regulated by estrogen alone [20], the mammary gland requires progesterone and prolactin in addition to estrogen to complete the architecture [12, 17, 33]. Ovariectomy and termination of weaning induce apoptosis in epithelial cells in the uterus, vagina and mammary gland [19, 30]. These estrogen target organs are controlled by estrogen receptors (ERα and ERβ) in the epithelial and stromal cells [9, 21, 24]. It is known, moreover, that growth factor(s) from the stroma are involved in epithelial proliferation of these organs [2, 6, 9]. An increase of epithelial and stromal cells in the uterus and vagina is mediated through *Insulin-like growth factor 1 (IGF-1)* and *Epidermal growth factor (EGF)* [3, 6, 14, 18]. Prolactin also induces expression of *Igf-2* mRNA in the developing mammary gland [13].

Tamoxifen, a selective ER modulator (SERM), acts as an estrogen agonist in the uterus and vagina, but acts as an estrogen antagonist in the mammary gland [22, 32]. The ligand-dependent effect on the mammary gland supports the idea of tissue specificity of gene expression by estrogen. Profiling of estrogen-regulated gene expression is reported recently in the estrogen target cells, tissues and organs [10, 34–36]. However, any comparisons of gene expression in the estrogen target organs have not not been reported. Gene expression reached a maximum 6 hr after E_2 administration in the uterus of ovariectomized adult mice without any histological changes [34]. Thus, we examined global gene expression 6 hr after a single injection of E_2 in order to identify early estrogen-responsive genes in the uterus vagina and mammary gland as the estrogen target organs in ovariectomized adult mice.

MATERIALS AND METHODS

Animals: C57BL/6J mice (CLEA, Tokyo, Japan) at 2 months of age, 20–23 g body weight, were used for mating. Mice were maintained under 12 hr light/12 hr dark at 23–25°C, fed with a commercial diet (CE-2, CLEA, Tokyo, Japan) and provided tap water *ad libitum*. All experiments

* CORRESPONDENCE TO: Prof. OHTA, Y., Laboratory of Experimental Animals, Department of Veterinary Medicine, Faculty of Agriculture, Tottori University, Koyama 680–8553, Japan.
e-mail: ohta@muses.tottori-u.ac.jp

and animal husbandry protocols were approved by the animal care committee of National Institutes of Natural Sciences.

Treatments: 17β-Estradiol (E_2, Sigma, St. Louis, MO) was dissolved in sesame oil. Sixty-day-old mice were ovariectomized and injected with 5 μg E_2/kg body weight after a 10-day recovery period to ensure that endogenous E_2 levels were reduced. Six hr after E_2 injection, 4 mice were killed by decapitation and the uteri, vaginae and mammary glands were collected. Four mice injected with oil vehicle only were used as controls. The tissues were pooled for DNA microarray analysis and the analyses were done on two independent experiments. Two other groups of 4 ovariectomized mice were likewise given E_2 or oil and killed 24 hr after the injection for bromodeoxyuridine (BrdU)-labeling study.

DNA microarray analysis: Total RNA was extracted from tissues (4 mice each) 6 hr after a single injection of 5 μg E_2/kg b.w. or the oil vehicle alone. Ten μg of total RNA were used to synthesize cDNA, which was then used to generate biotinylated cRNA. The cRNA was hybridized to murine U74A version 2 GeneChip expression arrays (Affymetrix, Applied Biosystems (APB), Tokyo, Japan) as described [34]. Total RNA was extracted using TRIzol reagent (Invitrogen, Tokyo, Japan) and purified with an RNeasy total RNA purification kit (Qiagen, Tokyo, Japan). Ten μg of total RNA were converted into double stranded cDNA using the Superscript Choice System (Invitrogen) with a T7-$(dT)_{24}$ primer (APB). Biotin-labeled cRNA was synthesized using the ENZO BioArray High Yield RNA transcript labeling kit (APB). The cRNA was purified by RNeasy (Qiagen). The purified cRNA was fragmented with fragmentation buffer (40 mM Tris, 100 mM K-acetate and 30 mM Mg-acetate) at 94°C for 35 min. Fragmented cRNA was mixed with hybridization buffer containing 100 mM MES [2-(N-morpholino)ethanesulfonic acid], 1 M NaCl, 20 mM EDTA, 0.01% Tween 20 and control oligonucleotides. The quality of cRNA was first assessed by analysis with Test 2 array (Affymetrix). cRNA was hybridized to Murine U74A version 2 GeneChip Expression Arrays (Affymetrix) for 16 hr at 45°C. All preparations were performed following manufacturer's instructions. Arrays were washed and stained with streptavidin-phycoerytherin, and scanned with an Argon-ion Laser Confocal Scanner (APB). Microarray analysis was performed twice on independent samples [34] and these raw data were loaded into NCBIs Gene Expression Omnibus as the dataset GSM159919-GSM159930 (GEO, http://www.ncbi.nlm.nih.gov/geo/). The putative target genes were validated by quantitative RT-PCR (QRT-PCR).

Statistical analysis: Signals in 2 experiments were detected using the robust multichip average (RMA) algorithms, and normalized using Genespring (Silicon Genetics, Redwoods City, CA). Expressed genes more than 40% raw signal of average raw signals in all genes on chip were selected as detected genes for next analysis. Selected genes showing more than 2-fold alterations by E_2 as compared to the tissue-matched oil controls were analyzed further using Genespring software.

Quantitative RT-PCR: One μg total RNA was reverse transcribed using Super Script II reverse transcriptase (Invitrogen) and random primers at 42°C for 50 min. PCR was performed using PE Prism 5,700 Sequence Detection System (PE Biosystems, Tokyo, Japan) with SYBR Green I dye (Molecular Probes, Eugene, OR) and primers selected by Primer Express *ver 1.0* (APB). Primer sets are described in Table 1.

PCR amplification was performed for 2 min at 50°C, for 10 min at 95°C and continued to 40 cycles at 95°C for 15 sec and at 60°C for 1 min. Data were normalized to ribosomal protein 28S RNA using delta Ct method for each primer set. The ratio was calculated as compared with oil controls of uterus.

BrdU-Labeling and Immunostaining: A single injection of 200 mg BrdU (Roche, Grenzacherstrasse, Switzerland)/kg b.w. was given to mice (4 mice each) 1 hr before sacrifice. Uterus, vagina and mammary gland were fixed with neutral-buffered 10% formalin, embedded in paraffin and sectioned at 6 μm. Sections were dipped in PBS and endogenous peroxidase activity was blocked with 3% H_2O_2 in methanol for 30 min. After washing in 0.5% Tween 20 in PBS twice, sections were dipped in 2N HCl for 20 min, then, neutralized sections borate buffer (0.1 M NaB_4O_7, pH 8.5) twice. After Tween/PBS washing, sections were dipped in 1% BSA/PBS for 20 min. Then, sections were incubated with 1:20 anti-BrdU (Roche). Sections detected with diaminobenzidine staining were analyzed. The BrdU labeling index (%) was estimated by counting BrdU positive cells in 2,000–3,000 epithelial and 10,000–20,000 stromal cells in the uterus and vagina, and in 300–500 epithelial or stromal cells in the mammary glands.

RESULTS

Gene expression in the uterus, vagina and mammary gland exposed to E_2: Approximately 12,400 genes were ana-

Table 1. Primer sets for QRT-PCR

Genebank accession No.	Name	Forward primer	Reverse primer
M13500	Klk 1	ATGGATGGAGGCAAAGACACTT	ACCTTGGAGAACACCATCACAGA
X04480	IGFI	CTACAAAAGCAGCCCGCTCTA	TCCTTCTGAGTCTTGGGCATGT
X81580	IGFBP2	GGAACATCTCTACTCCCTGCACAT	TTGTACCGGCCATGCTTGT
NM_010518	IGFBP5	GGTGTGTGGACAAGTACGGAATGA	ACGTTACTGCTGTCGAAGGCGT
X00525	Ribosomal 28S	AGACCGTCGTGAGACAGGTTAGTT	GCAGGATTACCATGGCAACAA

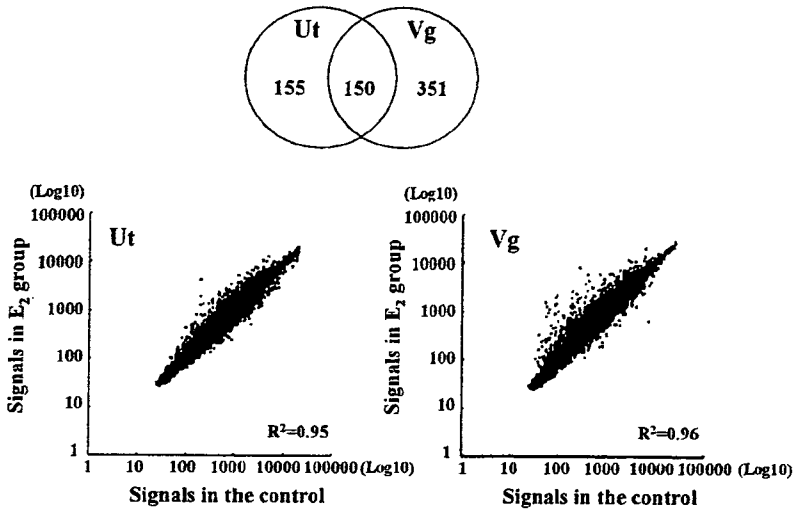

Fig. 1. Gene expression profiles in the uterus and vagina 6 hr after a single injection of 5 μg E_2/kg body weight. The Venn diagram indicatess detected genes in the oil-controls. Scatter plots indicate gene expression levels and the correlations between oil and E_2 groups in all genes. R_2 is correlation between oil and E_2 groups. Ut, uterus; Vg, vagina.

lyzed in the uterus, vagina and mammary gland. The total normalized signals between controls and E_2-exposed mice exhibited high correlations (R^2=0.95–0.96) (Fig. 1). The total number of genes showing at least 2-fold expression change 6 hr after a single injection of E_2 was 656 in all samples (Fig. 1). E_2 did not alter any gene expression more than 2-fold change in the mammary gland in the present study (data not shown). Genes showing organ-specific expression were 155 and 351 in the uterus and vagina, respectively (Fig. 1). Among them, 150 genes were regulated commonly in the uterus and vagina (Fig. 1).

In the uterus, 228 genes were up-regulated and 77 genes were down-regulated by E_2 as compared to the controls (Fig 2). In the vagina, 446 genes were up-regulated and 35 were down-regulated by E_2. In the uterus, 63% of E_2 up-regulated genes were overlapped those in the vagina. E_2 down-regulated common genes in the uterus and vagina were only 6 (Fig. 2). We further analyzed genes related to cell growth and organogenesis to find tissue-specific genes. E_2-responsive genes related to development, cell growth and apoptosis in the uterus and vagina were listed in Table 2.

Expression of Igf-1 family and Kallikrein 1 genes: Since clustering analysis revealed many E_2-regulated genes, we compared expressions of *Kallikrein 1 (Klk1)* genes and *Igf-1* family genes in each tissue using QRT-PCR.

In the controls, expression of *Klk1* mRNA was similar between uterus and vagina, while those of *Igf-1* and *Igfbp5* were lower in the vagina than in the uterus (Fig. 3). In the mammary gland, unlike the uterus and vagina, expressions of all mRNAs examined were very low or undetectable in the ovariectomized mice with or without E_2. In the uterus and vagina, expression of *Igf-1* mRNA was markedly increased by E_2. However, expressions of *Igfbp2* and *Igfbp5*

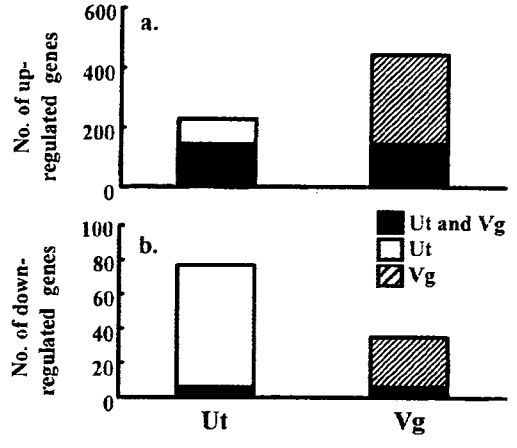

Fig. 2. Number of estrogen up-regulated genes (a) and down-regulated genes (b) in the uterus (Ut) and vagina (Vg). "Ut and Vg" indicates genes showing commonly altered expression by E_2 both in the uterus and vagina, while Ut and Vg indicate organ specific genes, respectively.

mRNAs were increased by E_2 in the vagina (Fig. 3). *Klk1* mRNAs was significantly increased as by E_2 in the vagina.

BrdU incorporation in the uterus, vagina and mammary gland, vagina 24 hr after E_2 injection: BrdU labeled cells were barely detected in epithelial cells of the uterus and mammary gland (0% and 0.05%) in the controls, as compared to those of the vagina (0.24%) in the controls (Fig. 4). The BrdU labeling index in the epithelial cells of the uterus and vagina was significantly increased 24 hr after the E_2 injection as compared with each control. In the mammary gland, however, BrdU-positive cells were not evident in the

Table 2. List of estrogen responsive genes related development, cell growth and apoptosis in the uterus and vagina by microarray analysis

Accession No.	Name	Ratio Ut	Ratio Vg
M60523	Inhibitor of DNA binding 3	**0.42**	0.71
AI840339	Ribonuclease, RNase A family 4	**0.42**	1.32
AA838868	Latent transforming growth factor beta binding protein 4	**0.42**	1.07
L31532	B-cell leukemia/lymphoma 2	**0.43**	0.59
X70298	SRY-box containing gene 4	**0.45**	**0.36**
U88567	Secreted frizzled-related protein 2	**0.45**	0.89
AI843106	Sestrin 1	**0.45**	**0.43**
AW123618	Frizzled homolog 2 (Drosophila)	**0.46**	0.64
AV092014	Peptidoglycan recognition protein 1	1.54	**0.37**
AI834950	Nuclear receptor subfamily 1, group D, member 1	0.58	**0.37**
AF076482	Peptidoglycan recognition protein 1	1.10	**0.40**
AF056187	IGF1 receptor	0.59	**0.41**
AF099973	Schlafen 2	1.02	**0.46**
X07750	Thyroid hormone receptor alpha	0.72	**0.49**
X81580	Insulin-like growth factor binding protein 2 (IGFBP2)	1.00	**2.00**
AW123099	Chromosome segregation 1-like (S. cerevisiae)	1.76	**2.01**
AF003695	Hypoxia inducible factor 1, alpha subunit	1.57	**2.01**
AI747899	Phosphatidylinositol transfer protein, beta	1.24	**2.02**
X03491	Keratin complex 2, basic, gene 4	1.03	**2.08**
X62154	similar to DNA replication licensing factor MCM3 (P1-MCM3)	1.48	**2.09**
AW124529	Tumor necrosis factor superfamily, member 5-induced protein 1	0.97	**2.16**
AF011644	CDK2 (cyclin-dependent kinase 2)-associated protein 1	1.81	**2.19**
AW048763	NMDA receptor-regulated gene 1	1.66	**2.20**
D49382	Septin 2	1.48	**2.20**
AW125478	HtrA serine peptidase 1	1.46	**2.22**
X02452	v-Ki-ras2 Kirsten rat sarcoma viral oncogene homolog	1.95	**2.26**
D10214	Prolactin receptor	1.12	**2.30**
AF014117	Glial cell line derived neurotrophic factor family receptor α 1	1.70	**2.34**
AF041476	Actin-like 6A	1.96	**2.36**
M73329	Protein disulfide isomerase associated 3	1.92	**2.38**
U35846	Apoptosis inhibitor 5	1.76	**2.43**
AF058798	Stratifin	1.32	**2.44**
D12780	S-adenosylmethionine decarboxylase 1	1.89	**2.47**
Z23077	S-adenosylmethionine decarboxylase 1 and 2	1.74	**2.49**
J04766	Plasminogen	1.02	**2.62**
D00613	Matrix Gla protein	0.63	**2.68**
X59846	Growth arrest specific 6	1.14	**2.79**
L12447	Insulin-like growth factor binding protein 5 (IGFBP5)	1.18	**3.09**
AI847054	Phosphatidic acid phosphatase type 2B	1.69	**3.32**
M35523	Cellular retinoic acid binding protein II	1.02	**3.47**
AI837110	Protein arginine N-methyltransferase 1	1.86	**3.49**
M74570	Aldehyde dehydrogenase family 1, subfamily A1	1.31	**4.11**
AV028204	Plasminogen	0.75	**4.38**
AI553024	Zinc finger and BTB domain containing 16	0.52	**4.44**
AW124889	Aldehyde dehydrogenase 18 family, member A1	**2.02**	1.45
AF100777	WNT1 inducible signaling pathway protein 1	**2.03**	1.38
AW260482	NMDA receptor-regulated gene 1	**2.10**	1.50
X13986	Secreted phosphoprotein 1	**2.17**	1.23
U00937	Growth arrest and DNA-damage-inducible 45 alpha	**2.18**	**3.08**
AF079528	Neuropilin 1	**2.20**	1.57
AB003502	G1 to S phase transition 1	**2.21**	1.66
D63784	DnaJ (Hsp40) homolog, subfamily C, member 2	**2.24**	1.96
AI645561	NMDA receptor-regulated gene 1	**2.29**	**2.10**
U53208	DnaJ (Hsp40) homolog, subfamily C, member 2	**2.34**	1.79
AW046181	Serum/glucocorticoid regulated kinase	**2.38**	1.02
AA529583	Mortality factor 4 like 2	**2.39**	**3.56**
V00756	Interferon-related developmental regulator 1	**2.40**	**2.63**
U88327	Suppressor of cytokine signaling 2	**2.42**	1.07
AB012276	Activating transcription factor 5	**2.43**	1.96
M13500	Kallikrein 1	**2.43**	0.92

Table 2. Continued

Accession No.	Name	Ratio Ut	Ratio Vg
U84411	Protein tyrosine phosphatase 4a1	**2.46**	**2.34**
AW048937	Cyclin-dependent kinase inhibitor 1A (P21)	**2.51**	**2.45**
AF055638	Growth arrest and DNA-damage-inducible 45 gamma	**2.53**	**5.03**
AI596034	Receptor tyrosine kinase-like orphan receptor 2	**2.64**	**3.31**
V00727	FBJ osteosarcoma oncogene	**2.66**	**3.22**
L32751	RAN, member RAS oncogene family	**2.77**	**2.36**
D50086	Neuropilin 1	**2.95**	1.27
X99273	Aldehyde dehydrogenase family 1, subfamily A2	**2.99**	1.90
M63801	Gap junction membrane channel protein alpha 1	**3.02**	1.98
AI785289	Guanine nucleotide binding protein-like 3 (nucleolar)	**3.82**	**2.57**
X04480	Insulin-like growth factor 1 (IGF-I)	**4.67**	**4.82**
U83902	MAD2 (mitotic arrest deficient, homolog)-like 1 (yeast)	**4.75**	**4.57**
AF053232	Nucleolar protein 5	**5.09**	**3.32**
X69620	Inhibin beta-B	**10.29**	**7.60**

Bold means more than 2-fold alterations by E_2.

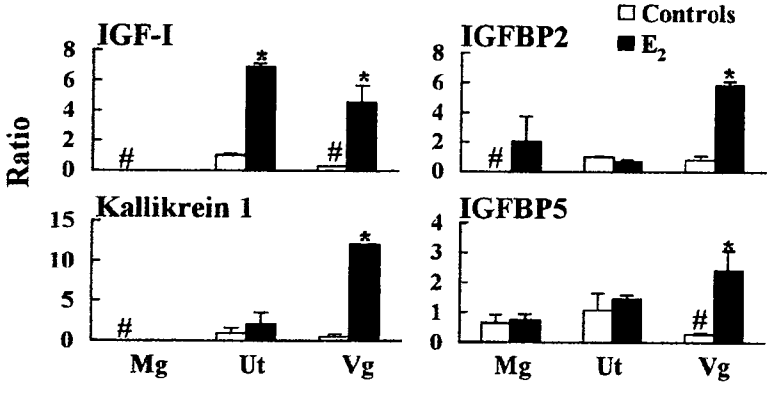

Fig. 3. Ratio of mRNA gene expressions of *Igf-1* family and *Kallikrein 1* in the three organs 6 hr after the E_2 injection using QRT-PCR. *, $P<0.05$ v.s. the control of each tissue; #, $P<0.05$ v.s. the control uterus.

epithelium 24 hr after the E_2 injection. The index was significantly increased by E_2 in the uterine stroma (Fig. 4).

DISCUSSION

Estrogen regulates mitosis and morphological changes in female reproductive organs during proliferative events, such as estrous cycles, gestation and lactation. In order to understand the underlying mechanisms of estrogen functions in reproductive organs, detection of estrogen responsive genes in each reproductive organs are is essential. Effects of estrogen are different in each reproductive organ, therefore we investigated a global gene expression in uterus, vagina and mammary gland after a single injection of E_2.

In the present study, BrdU labeled cells were remarkably increased in the uterine and vaginal epithelia, and in the uterine stroma after the E_2 injection, but not in any parts of the mammary gland. Gene expression in response to estrogen is different among these organs. *Igf-1* is a key epithelial mitogen induced by estrogenic chemicals [28, 31], whereas IGFBP prevents signal pathway by binding to *Igf-1*, and inhibits phosphorlylation of Insulin receptor substrate-1 (IRS-1), Phosphatidylinositol 3-kinase (PI3K), Protein kinase B (PKB) and Forkhead transcription factors (FKHRL1) [23]. *Igfbp2* and *Igfbp5* promote apoptosis in the prostate cancer cells and mammary gland cells [23, 26, 27, 29]. Hence, proliferations of uterine and vaginal cells was appear to be regulated by estrogen via *Igf-1* and receptor complex, and its modulator. In the present study, estrogen increased *Igf-1* mRNA and mitosis in the uterus and vagina. However, the *Igf-1* modulators and *Igfbp* mRNAs were also increased in E_2-exposed vagina. This may be accounted for by the suppression of stromal cell proliferation caused by increase of *Igfbp* mRNAs in the stroma rather than the epithelium. Up-regulation of *Klk1* was reported by E_2 in the uterus [34]. *Klk* plays an important role for the release of bradykinin from kininogen, activation of growth factors and alteration of the extracellular matrix in the uterine epithelium [7]. *Klk* is regulated hormonally [7, 8] and the gene expression was found in human ovarian, prostate

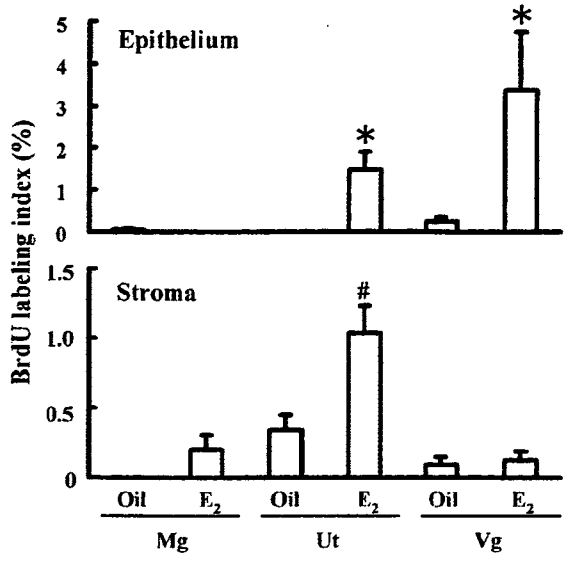

Fig. 4. BrdU labeling index (positive cells/counted cells, %) in epithelium and stroma of the mammary gland, uterus and vagina. Mg, mammary gland; Ut, uterus; Vg, vagina; *, $P<0.05$ v.s. the control of each tissue.

and breast cancer cells and in mouse vagina [15, 25, 37]. We found the up-regulation of *Klk1* gene expression in the vagina by QRT-PCR. Thus, *Klk1* may be related to epidermal proliferation and their expressions can be used for markers of acute response to estrogen in the uterus and vagina.

We found that estrogen regulated genes were markedly limited in the mammary gland as compared to those in the uterus and vagina 6 hr after the E_2 exposure. Global gene expression in E_2-exposed mammary gland has not been reported. Only gene expression in human breast cancer MCF-7 cells treated E_2 *in vitro* was reported [4, 10, 11]. MCF-7 cells treated with E_2 revealed the major down-regulation (70%) of gene expression including transcriptional repressor, antiproliferative and proapoptotic genes, such as *Bcl-2, Cyclin G2* and *TGF-β* family [11]. Moreover, using the serial analysis of gene expression (SAGE) method, 3 up-regulated genes were reported in MCF-7 cells 10 hr after E_2 treatment *in vitro* [4]. The genes reported as E_2 down-regulated genes in MCF-7 cells were not found in the mammary gland in the present study. MCF-7 cells are a single species of mammary cancer cells and show precise response of time- and dose-dependent proliferation to estrogen. Normal mammary gland may need longer than 6 hr to respond to E_2 *in vivo*. Mammary gland has various types of cells, such as epithelial cells stromal cells and adipocytes. Thus, we need further precise experiment to understand estrogen responsive genes in the mammary gland.

Although the mammary gland is known to be one of the target organs of estrogen, ER-α knockout (αERKO) mice showed proliferation and morphogenesis of the mammary gland in adulthood [24]. The mammary gland seems to be regulated by progesterone and prolactin rather than estrogen [5, 12, 15, 17, 24, 33]. The up-regulation of gene expression, such as *IRS-1, Msx-2, C/EBPβ* and *Stat5*, by progesterone was reported in human breast cancer cells [15]. Prolactin induced expression of *Igf-2* mRNA in the developing mammary gland [13]. Thus, mammary gland is possibly regulated largely by progesterone and/or prolactin. This may account for no expression of estrogen responsive genes observed 6 hr after the E_2 exposure and absence of definite mitogenic response in the mammary gland of ovariectomized adult mice 24 hr after the E_2 exposure.

In conclusion, E_2 regulates expression of a number of genes in the vagina and uterus, but not in the mammary gland. Half of E_2-regulated genes in the uterus were in common with the vagina including *Kallikrein* and *Igf* family genes. Differences in expression of these genes in response to E_2 may be leased on the tissue specificity to estrogen exposure. The candidate estrogen responsive genes in the uterus and vagina identified by profiling provide an important foundation to understand functional mechanisms of estrogen regulating morphogenesis and maintenance of the reproductive organ.

ACKNOWLEDGMENTS. We are grateful to Prof. N. Takasugi for his critical reading of this manuscript. This work was supported in part by a grant-in-aid for Scientific Research from the Ministry of Education, Culture, Sports, Science and Technology of Japan, and Health Sciences Research Grant from the Ministry of Health, Labor and Welfare, and a Research Grant from the Ministry of Environment, Japan.

REFERENCES

1. Bolstad, B., Irizarry, R., Astrand, M. and Speed, T. 2003. A comparison of normalization methods for high density oligonucleotide arra data based on variance and bias. *Bioinformatics* **16**: 185–193.
2. Buchanan, D.L., Kurita, T., Taylor, J.A., Lubahn, D.B., Cunha, G.R. and Cooke, P.S. 1998. Role of stromal and epithelial estrogen receptors in vaginal epithelial proliferation, stratification, and cornification. *Endocrinology* **139**: 4345–4352.
3. Buchanan, D.L., Setiawan, T., Lubahn, D.B., Taylor, J.A., Kurita, T., Cunha, G.R. and Cooke, P.S. 1999. Tissue compartment-specific estrogen receptor-alpha participation in the uterine epithelial secretory response. *Endocrinology* **140**: 484–491.
4. Charpentier, A.H., Bednarek, A.K., Daniel, R.L., Hawkins, K.A., Laflin, K.J., Gaddis, S., MacLeod, M.C. and Aldaz, C.M. 2000. Effects of estrogen on global gene expression: identification of novel targets of estrogen action. *Cancer Res.* **60**: 5977–5983.
5. Clevenger, C.V., Furth, P.A., Hankinson, S.E. and Schuler, L.A. 2003. The role of prolactin in mammary carcinoma. *Endocr. Rev.* **24**: 1–27.
6. Cooke, P.S., Buchanan, D.L., Young, P., Setiawan, T., Brody, J., Korach, K.S., Taylor, J., Lubahn, D.B. and Cunha, G.R. 1997. Stromal estrogen receptors mediate mitogenic effects of estradiol on uterine epithelium. *Proc. Natl. Acad. Sci. U.S.A.* **94**: 6535–6540.
7. Corthorn, J. and Valdes, G. 1994. Variations in uterine kal-

likrein during cycle and early pregnancy in the rat. *Biol. Reprod.* **50**: 1261–1264.
8. Corthorn, J., Figueroa, C. and Valdes, G. 1997. Estrogen and luminal stimulation of rat uterine kallikrein. *Biol. Reprod.* **56**: 1432–1438.
9. Cunha, G.R., Young, P., Hom, Y.K., Cooke, P.S., Taylor, J.A. and Lubhan, D.B. 1997. Elucidation of a role of stromal steroid hormone receptors in mammary gland growth and development by tissue recombination experiments. *J. Mammary Gland Biol. Neoplasia* **2**: 393–402.
10. Frasor, J., Danes, J.M., Komm, B., Chang, K.C., Lyttle, C.R. and Katzenellenbogen, B.S. 2003. Profiling of estrogen up- and down-regulated gene expression in human breast cancer cells: insights into gene networks and pathways underlying estrogenic control of proliferation and cell phenotype. *Endocrinology* **144**: 4562–4574.
11. Gruvberger, S., Ringner, M., Chen, Y., Panavally, S., Saal, L.H., Borg, A., Ferno, M., Peterson, C. and Meltzer, P.S. 2001. Estrogen receptor status in breast cancer is associated with remarkably distinct gene expression patterns. *Cancer Res.* **61**: 5979–5984.
12. Horseman, N.D. 1999. Prolactin and mammary gland development. *J. Mammary Gland Biol. Neoplasia* **4**: 79–88.
13. Hovey, R.C., Harris, J., Hadsell, D.L., Lee, A.V., Ormandy, C.J. and Vonderhaar, B.K. 2003. Local insulin-like growth factor-II mediates prolactin-induced mammary gland development. *Mol. Endocrinol.* **17**: 460–471.
14. Huet-Hudson, Y.M., Chakraborty, C., De, S.K., Suzuki, Y., Andrews, G.K. and Dey, S.K. 1990. Estrogen regulates the synthesis of epidermal growth factor in uterine epithelial cells. *Mol. Endocrinol.* **4**: 510–523.
15. Jacobsen, B.M., Richer, J.K., Sartorius, C.A. and Horwitz, K.B. 2003. Expression profiling of human breast cancers and gene regulation by progesterone receptors. *J. Mammary Gland Biol. Neoplasia* **8**: 257–268.
16. Katsu, Y., Takasu, E. and Iguchi, T. 2002. Estrogen-independent expression of neuropsin, a serine protease in the vagina of mice exposed neonatally to diethylstilbestrol. *Mol. Cell Endocrinol.* **195**: 99–107.
17. Kelly, P.A., Bachelot, A., Kedzia, C., Hennighausen, L., Ormandy, C.J., Kopchick, J.J. and Binart, N. 2002. The role of prolactin and growth hormone in mammary gland development. *Mol. Cell Endocrinol.* **197**: 127–131.
18. Klotz, D.M., Hewitt, S.C., Ciana, P., Raviscioni, M., Lindzey, J.K., Foley, J., Maggi, A., DiAugustine, R.P. and Korach, K.S. 2002. Requirement of estrogen receptor-alpha in insulin-like growth factor-1 (IGF-1)-induced uterine responses and *in vivo* evidence for IGF-1/estrogen receptor cross-talk. *J. Biol. Chem.* **277**: 8531–8537.
19. Kojima, H., Fukazawa, Y., Sato, T., Enari, M., Tomooka, Y., Matsuzawa, A., Ohta, Y. and Iguchi, T. 1996. Involvement of the TNF-α system and the Fas system in the induction of apoptosis of mammary glands after weaning. *Apoptosis* **1**: 201–208.
20. Korach, K.S., Couse, J.F., Curtis, S.W., Washburn, T.F., Lindzey, J., Kimbro, K.S., Eddy, E.M., Migliaccio, S., Snedeker, S.M., Lubahn, D.B., Schomberg, D.W. and Smith, E.P. 1996. Estrogen receptor gene disruption: molecular characterization and experimental and clinical phenotypes. *Recent Prog. Horm. Res.* **51**: 159–188.
21. Kurita, T., Lee, K.J., Cooke, P.S., Taylor, J.A., Lubahn, D.B. and Cunha, G.R. 2000. Paracrine regulation of epithelial progesterone receptor by estradiol in the female reproductive tract. *Biol. Reprod.* **62**: 821–830.
22. Margeat, E., Bourdoncle, A., Margueron, R., Poujol, N., Cavailles, V. and Royer, C. 2003. Ligands differentially modulate the protein interactions of the human estrogen receptors alpha and beta. *J. Mol. Biol.* **326**: 77–92.
23. Marshman, E., Green, K.A., Flint, D.J., White, A., Streuli, C.H. and Westwood, M. 2003. Insulin-like growth factor binding protein 5 and apoptosis in mammary epithelial cells. *J. Cell Sci.* **116**: 675–682.
24. Mueller, S.O., Clark, J.A., Myers, P.H. and Korach, K.S. 2002. Mammary gland development in adult mice requires epithelial and stromal estrogen receptor alpha. *Endocrinology* **143**: 2357–2365.
25. Obiezu, C.V., Scorilas, A., Katsaros, D., Massobrio, M., Yousef, G.M., Fracchioli, S., Rigault, de la Longrais, I.A., Arisio, R. and Diamandis, E.P. 2001. Higher human kallikrein gene 4 (KLK4) expression indicates poor prognosis of ovarian cancer patients. *Clin. Cancer Res.* **7**: 2380–2386.
26. Plath-Gabler, A., Gabler, C., Sinowatz, F., Berisha, B. and Shams, D. 2001. The expression of the IGF family and GH receptor in the bovine mammary gland. *J. Endocr.* **160**: 39–48.
27. Schneider, M.R., Wolf, E., Hoeflich, A. and Lahm, H. 2002. IGF-binding protein-5: flexible player in the IGF system and effector on its own. *J. Endocr.* **172**: 423–440.
28. Richards, R.G., DiAugustine, R.P., Petrusz, P., Clark, G.C. and Sebastian, J. 1996. Estradiol stimulates tyrosine phosphorylation of the insulin-like growth factor-1 receptor and insulin receptor substrate-1 in the uterus. *Proc. Natl. Acad. Sci. U.S.A.* **93**: 12002–12007.
29. Richardsen, E., Ukkonen, T., Bjornsen, T., Mortensen, E., Egevad, L. and Busch, C. 2003. Overexpression of IGBFB2 is a marker for malignant transformation in prostate epithelium. *Virchows Arch.* **442**: 329–335.
30. Sato, T., Fukazawa, Y., Kojima, H., Enari, M., Iguchi, T. and Ohta, Y. 1997. Apoptotic cell death during the estrous cycle in the rat uterus and vagina. *Anat. Rec.* **248**: 76–83.
31. Sato, T., Wang, G., Hardy, P.M., Kurita, T., Cunha, G.R. and Cooke, P.S. 2002. Role of systemic and local *IGF-1* in the effects of estrogen on growth and epithelial proliferation of uterus. *Endocrinology* **143**: 2673–2679.
32. Shang, Y. and Brown, M. 2002. Molecular determinants for the tissue specificity of SERMs. *Science* **295**: 2465–2468.
33. Shyamala, G. 1999. Progesterone signaling and mammary gland morphogenesis. *J. Mammary Gland Biol. Neoplasia* **4**: 89–104.
34. Watanabe, H., Suzuki, A., Mizutani, T., Khono, S., Lubahn, D.B., Handa, H. and Iguchi, T. 2002. Genome-wide analysis of changes in early gene expression induced by oestrogen. *Genes Cells* **7**: 497–507.
35. Watanabe, H., Suzuki, A., Kobayashi, M., Takahashi, E., Itamoto, M., Lubahn, D.B., Handa. H. and Iguchi, T. 2003. Analysis of temporal changes in the expression of estrogen-regulated genes in the uterus. *J. Mol. Endocrinol.* **30**: 347–358.
36. Watanabe, H., Suzuki, A., Kobayashi, M., Lubahn, D.B., Handa, H. and Iguchi, T. 2003. Similarities and differences in uterine gene expression patterns caused by treatment with physiological and non-physiological estrogen. *J. Mol. Endocr.* **31**: 487–497.
37. Yousef, G.M., Obiezu, C.V., Luo, L.Y., Black, M.H. and Diamandis, E.P. 1999. Prostase/KLK-L1 is a new member of the human kallikrein gene family, is expressed in prostate and breast tissues, and is hormonally regulated. *Cancer Res.* **59**: 4252–4256.